https://doi.org/10.5194/nhess-2023-111
Preprint. Discussion started: 18 July 2023


Natural Hazards and Earth System Sciences
Discussions

# An estimate of excess mortality resulting from air pollution caused by wildfires in the eastern and central Mediterranean basin in 2021

Bin Zhou[1,2] and Christoph Knote[1]

[1]Model-based Environmental Exposure Science, Faculty of Medicine, University of Augsburg, Universitätsstraße 2, 86159, Augsburg, Bavaria, Germany
[2]Potsdam Institute for Climate Impact Research (PIK), Member of the Leibniz Association, Telegrafenberg A31, 14473, Potsdam, Brandenburg, Germany

**Correspondence:** Bin Zhou (bin.zhou@med.uni-augsburg.de)

**Abstract.** Wildfires result in human fatalities not only due to the direct exposure to flames, but also indirectly through smoke inhalation. The Mediterranean basin with its hot and dry summers is a hotspot for such devastating events. The situation has further been aggravated in recent years by climate change as well as a growing and aging population in the region. To assess the health impacts due to short-term exposure to air pollution created by the 2021 summer wildfires in the eastern and central Mediterranean basin, we used a regional-scale chemistry transport model to simulate concentrations of major air pollutants such as fine particulate matter with an aerodynamic diameter less than 2.5 $\mu$m ($PM_{2.5}$), $SO_2$, $NO_2$, and $O_3$ - in a fire and a no-fire scenario. Elevated short-term exposure of the population to air pollutants are associated with excess all-cause mortality using relative risks (RRs) for individual pollutants from previously published meta-analyses. Our estimates indicate that the short-term exposure to wildfire-caused changes in $O_3$ accounted for 289 (95% CI:214-364) excess deaths in total over the entire region of investigation during the wildfire season between mid-July to early October 2021. This is followed by 87 (95% CI: 56 - 118) excess deaths due to elevated $PM_{2.5}$ exposure, rendering the health effect of increased $O_3$ from wildfires larger than the effect of increased $PM_{2.5}$. We attributed this largely to the spatially more widespread impact of wildfires on $O_3$. Our study concludes with a discussion on uncertainties associated with the health impact assessment based on different air pollutants.

## 1 Introduction

Air pollution is a central issue in public health globally given its well-documented association with adverse health effects (Brunekreef and Holgate, 2002; Anenberg et al., 2010; Lelieveld et al., 2020). Exposure to air pollution, both long-term and short-term, is estimated to cause millions of premature deaths and lost years of healthy life each year (WHO, 2021). Air pollution caused by wildfires is becoming a subject of increasing concern due to the higher toxicity associated with its chemical composition (Naeher et al., 2007; Wegesser et al., 2009).

https://doi.org/10.5194/nhess-2023-111
Preprint. Discussion started: 18 July 2023


Natural Hazards and Earth System Sciences
Discussions

Wildfires emit large amounts of particulate matter (PM), nitrogen oxides ($NO_x$), as well as carbon monoxide (CO) and volatile organic compounds (VOCs) into the atmosphere (Schneider and Abbatt, 2022). Wildfires increase PM levels through direct emission of particles as well as the formation of secondary PM from the oxidation of the emitted ammonia ($NH_3$), $SO_2$, $NO_x$, and VOCs. These species are oxidized to less volatile sulfates, nitrates, and secondary organic aerosols, respectively, which then condense onto pre-existing particles or form new ones (Kroll et al., 2020). Some VOCs are in part emitted with semi- and low volatility and will condense onto particles upon dilution and cooling without the need of further photochemical reactions.

Increased $NO_x$ and VOCs from wildfires lead to additional ozone ($O_3$) formation downwind through photo-chemical reactions (Jaffe and Wigder, 2012), as well as increases in the concentrations of the hydroxyl radical (OH). The reader is referred to Xu et al. (2021) for a summary of observational evidence from a large recent airborne field campaign. Both increases result in an increased atmospheric oxidation capacity, which in turn further favors the formation of secondary PM (Hobbs et al., 2003; Akagi et al., 2011).

Smoke from wildfires can travel large distances and affect the health of a much larger population than the effects of the actual fire (Bencherif et al., 2020). Most recently, prominent examples are wildfires in the Amazon in 2019 (Butt et al., 2021), Australia in 2019-2020 (Graham et al., 2021), and those in the United States in recent years (Burke et al., 2021; Kramer et al., 2019; Xie et al., 2020). It has been shown that frequency and magnitude of fire events are increasingly affected by human activities and have been exacerbated by climate change (Bowman et al., 2020; Jolly et al., 2015).

Globally, wildfire smoke is estimated to cause more than 330,000 premature deaths each year during 1997 - 2006 (Johnston et al., 2012). This is traditionally considered to be dominated by the effects of inhaling (fine) particulate matter (e.g., Fann et al., 2018). As climate change worsens, together with updated evidence of impacts of wildfires on human health (Chen et al., 2021; Haikerwal et al., 2015), wildfires are projected to result in increased human and material losses in the near future (Xu et al., 2020). Furthermore, wildfires can lead to a higher susceptibility to other (respiratory) diseases, with reports of an amplified risk of COVID-19 cases and deaths in wildfire seasons (Zhou et al., 2021; Schwarz et al., 2022) as a prime example. This may imply that previous studies may systematically underestimate the actual health impacts of wildfires, as they fail to adequately address the underlying relationship between wildfires and other environmental and health concerns.

Historically, the Mediterranean basin which is characterized by hot and dry summers has been negatively affected by wildfires. With increased warming and declining precipitation, the Mediterranean basin is expected to experience an increase in the frequency and scale of wildfires (Ruffault et al., 2020; Cos et al., 2021). Meanwhile, the rapid population growth in some countries (e.g., Egypt, Israel, and Tunisia) and an ageing population in others (e.g., southern European countries) renders the Mediterranean basin ever more vulnerable to the unfavorable consequences of climate change (Linares et al., 2020). All this demands a comprehensive assessment of population exposure to wildfire-caused air pollution.

In this context, the 2021 summer wildfires in the eastern and central Mediterranean basin serve as an indicator of future wildfire impacts. In our work we used this case to assess the health impacts due to short-term exposure to air pollution from wildfire smoke. An online-coupled atmospheric chemistry transport model was employed to simulate concentrations of major air pollutants – fine particulate matter with a diameter of 2.5 $\mu$m or less ($PM_{2.5}$), $SO_2$, $NO_2$, and $O_3$ – in a fire and a no-fire

https://doi.org/10.5194/nhess-2023-111
Preprint. Discussion started: 18 July 2023


Natural Hazards and Earth System Sciences
Discussions

scenario. Elevated short-term exposure to air pollutants are associated with excess all-age all-cause mortality using relative risks (RRs) for individual pollutants based on previously published meta-analyses. We estimated the excess mortality attributable to wildfires for the entire region and the countries included, with detailed discussions on the uncertainties associated with the estimates.

## 2 Data and Methods

### 2.1 Study area and period

The study area covers 18 countries and regions in the central and eastern Mediterranean basin with a total population of 334.62 million in 2020, of which over half resides along its coastal areas and hydrological basins (World Bank, 2020). For a full list of countries included in the study and their respective populations, please refer to Tab. A1 in Appendix A.

We used the UN WPP-Adjusted population count GPWv4 dataset of the Gridded Population of the World, Version 4 (GPWv4) data from the Socioeconomic Data and Application Center (SEDAC) for 2020 (CIESIN, 2018) to describe the spatial population distribution. From the original resolution of 2.5 arc-minute (approx. 5 km) data were aggregated to a grid of about 20 x 20 $km^2$ to be consistent with the configuration of the numerical model employed in this study (Fig. 1a).

The study period was 15 July - 02 October 2021, covering the major wildfire events in summer 2021. The severe dry conditions and heatwaves prevailing in this period have resulted in many intense and long-lasting wildfires across the region, emitting large amounts of air pollutants, e.g., PM, $NO_x$, and $SO_2$ into the atmosphere (CAMS, 2021). According to the European Forest Fire Information System (EFFIS) (EFFIS, 2021), there were more than 1800 wildfires with a burnt area of 10 hectares or larger occurring in the region and period of this study, which burnt 589,400 hectares area in total. This makes 2021 the second worst fire season in the European Union since 2000, surpassed only by 2017 (San-Miguel-Ayanz et al., 2022). As shown in Fig. 1 b-c, the worst hit countries include Turkey, Greece, Italy, Tunisia, and in the Balkans (e.g., Albania, Montenegro, and North Macedonia).

### 2.2 Model description

Concentrations of $PM_{2.5}$, $O_3$, $NO_2$, and $SO_2$ were simulated using the Weather Research and Forecasting model coupled to Chemistry (WRF-Chem) model (version 4.2.1), a fully online-coupled regional atmospheric chemistry model (Grell et al., 2005). The Model for Ozone and Related chemical Tracers, version 4 (MOZART-4) gas-phase chemistry mechanism (Emmons et al., 2010) with considerable updates to the chemistry of VOCs (Knote et al., 2014) was used to predict trace gas concentrations. Aerosol characteristics were simulated with the 4 size-bin implementation of the MOSAIC aerosol module (Zaveri et al., 2008). This includes a simplified formulation of secondary organic aerosol formation (Hodzic and Jimenez, 2011), including that from wildfires.

Analyses interlaced with hourly forecasts from the Global Forecasting System (GFS) of the National Centers for Environmental Prediction (NCEP) made available through the NOAA Operational Model Archive and Distribution System (NOMADS,

https://doi.org/10.5194/nhess-2023-111
Preprint. Discussion started: 18 July 2023


Natural Hazards and Earth System Sciences
Discussions

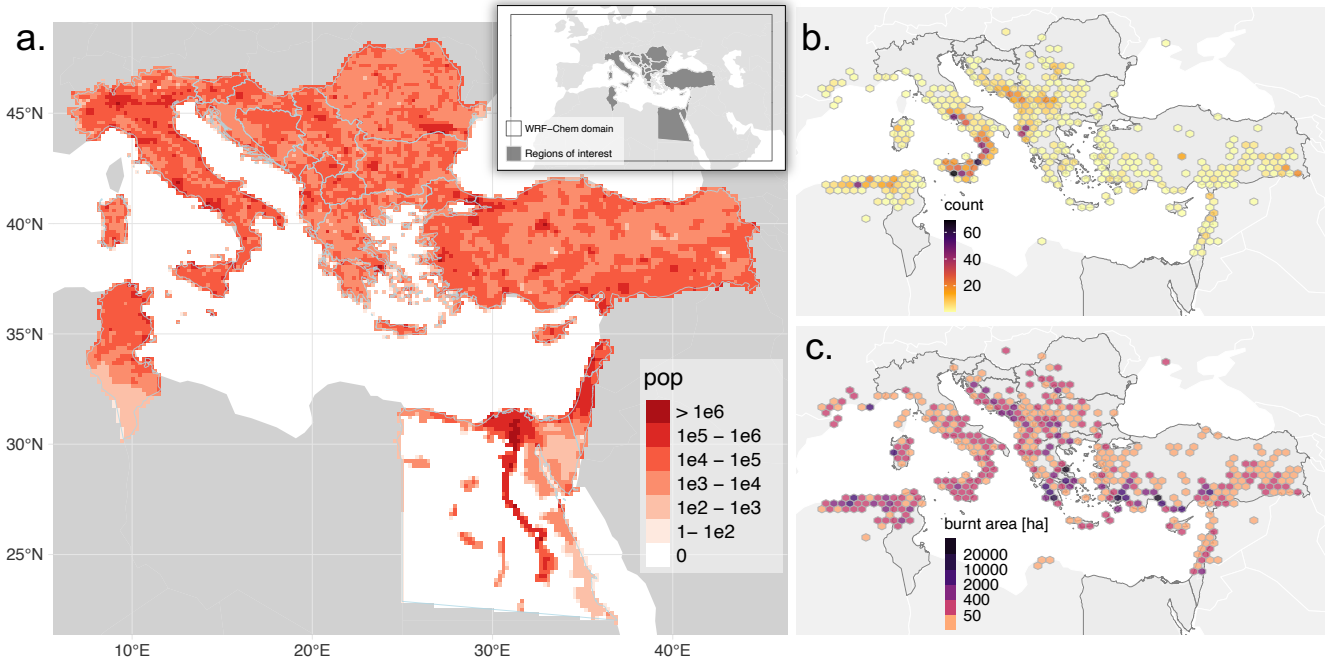


**Figure 1.** The study region overlaid with the population data and wildfire statistics. a) Population counts per country from the Gridded Population of the World, Version 4 (GPWv4) data for 2020 (CIESIN, 2018). The light gray rectangle in the inlet demarcates the simulation domain. b-c) the total number of wildfires and total burnt areas, respectively, based on the European Forest Fire Information System (EFFIS) data between 15-July and 02-October, 2021. Countries included in the study are outlined in black.

(Rutledge et al., 2006)) were used as initial and boundary conditions for meteorological variables. Simulations from the Whole Atmosphere Community Climate Model (WACCM) model created by the Atmospheric Chemistry Observations & Modeling Laboratory (ACOM) of the National Center of Atmospheric Research (NCAR) served to provide initial and boundary conditions for trace gases and particles (https://www.acom.ucar.edu/waccm/, last accessed 02.03.2022).

The EDGAR v5.0 dataset was used for prescribing anthropogenic emissions (Crippa et al., 2021). The model simulations also considered biogenic emissions from plants (Guenther et al., 2006), desert dust (LeGrand et al., 2019) and sea spray (Gong, 2003). Emissions of trace gases and particles from wildfires were included by the Fire INventory from NCAR (FINN) model (Wiedinmyer et al., 2011) in version 1.5, based on daily observations by the MODIS and VIIRS satellite instruments. The plume-rise scheme used is originally based on Freitas et al. (2007). Archer-Nicholls et al. (2015) have coupled it to the MOSAIC aerosol scheme also used in this work, and evaluated it for biomass burning episodes in Brazil. As part of Knote et al. (2014) and Knote et al. (2015) we made sure to extend this coupling to the improved MOZART gas-phase mechanism and MOSAIC scheme described therein. Secondary organic aerosol formation from biomass burning is considered using the observationally-constrained approach described in (Hodzic and Jimenez, 2011).

https://doi.org/10.5194/nhess-2023-111
Preprint. Discussion started: 18 July 2023


Natural Hazards and Earth System Sciences
Discussions

This model configuration has already been evaluated in different regions of the world and used to simulate the concentrations of various air pollutants (Graham et al., 2021; Butt et al., 2021).

The model domain in this study covers the central and eastern Mediterranean basin (24.54° W - 63.54° E, 16.95 - 56.57° N) at 20 km horizontal resolution, with 33 vertical levels (up to 10 hPa) (Fig. 1a). Model meteorology was re-initialized every 48 hours with meteorological analyses from GFS, and then allowed to be evolved freely within the boundary layer. Above the boundary layer, grid nudging was performed to keep mesoscale features in line with GFS analyses. Aerosol and trace gas fields were carried over without re-initialization between runs. This setup had been developed previously to strike an optimal balance between realistically considering aerosol-radiation and aerosol-cloud interactions whilst also keeping in line with actual weather development (Im et al., 2015b).

Two simulations, a fire and a no-fire scenario, were performed to quantify the contribution of wildfires to concentrations of major air pollutants.

### 2.3 Model evaluation

We used the European Environmental Agency (EEA)'s AirBase air quality (including $PM_{2.5}$, $O_3$, $NO_2$, and $SO_2$) time series data sets (E1a & E2a) to evaluate the WRF-Chem simulations. AirBase data reported by EEA's member states are provided either at hourly or daily intervals. Based on type and location, AirBase stations are classified as rural (including "rural-remote", "rural-regional"), sub-urban (including "rural-nearcity"), and urban. All AirBase data are quality-checked and flagged with different levels of verification (European Environment Agency, 2021). We only used data with "verification code" equal to 1 (verified) or 2 (preliminary verified) in the metadata, and only from stations where more than 75% of observations were present during the entire period. Nevertheless, the verified data from each AirBase station could still contain outliers which we defined as observations with four standard deviations from its mean over the entire study period and were thus removed. For stations where only daily means were recorded, hourly WRF-Chem values were averaged to daily means for comparison. The data were downloaded using `airbase 0.2.7` python library (https://pypi.org/project/airbase/).

For WRF-Chem simulations of each air pollutant, the conventional statistical metrics, such as mean bias (MB), normalized mean bias (NMB), root mean square error (RMSE), and index of agreement (IOA), were calculated (see Tab. B1). In addition, Taylor diagrams (Taylor, 2001) were plotted to compare the model's performance at different locations (rural, suburban, and urban) and averaging frequencies (daily versus hourly mean).

### 2.4 Health impacts assessment (HIA)

Health impacts of short-term exposure to wildfire-caused air pollution were estimated using a well-established methodology (WHO, 2016). Details of the main steps are given below.

https://doi.org/10.5194/nhess-2023-111
Preprint. Discussion started: 18 July 2023


Natural Hazards and Earth System Sciences
Discussions

#### 2.4.1 Determination of population exposure to air pollution

Population exposure was quantified for each country by calculating the population-weighted concentrations of air pollutants using GWPv4 population data and pollutant concentration data from the WRF-Chem simulations. For country $J$ on day $d$, its population weighted exposure ($Cp$) to a pollutant $i$ - say, $i$ is $PM_{2.5}$, is then calculated as:

$$Cp_{i,J,d} = \frac{\sum_{\forall j \in J} (pop_j \times c_{i,j,d})}{\sum_{\forall j \in J} pop_j} \quad (1)$$

where $pop_j$ is the population counts in any grid cell $j$ pertaining to country $J$; $c_{i,j,d}$ is the daily mean air pollutant concentration for $PM_{2.5}$, $SO_2$, and $NO_2$, whereas the daily maximum 8 hour average (DMA8) is used for $O_3$. Population-weighted exposure was computed for both fire and non-fire scenarios, with their difference representing the additional health burden attributable to wildfires.

#### 2.4.2 Estimate of exposure-associated health risk

To estimate the exposure-associated health risk, we used both baseline health statistics (here e.g., mortality) and an exposure-response-function (ERF) for individual air pollutants.

The baseline all-cause mortality data in both genders (deaths per annum) for 2019 (the latest year for which data are available) were downloaded from the Global Health Data Exchange (GHDx) (Global Burden of Disease Collaborative Network, 2020). As shown in Fig. A1, the annual mortality rates of countries range from 515 (Israel) to 1791 (Bulgaria) deaths per 100,000 population. To interpolate the annual deaths to the summer months (July-August-September) 2021, we used the multi-annual (2010-2019) average of monthly deaths as proxy. Monthly baseline mortality data are collected by the European Statistical Office (Eurostat) for its member and associated states (Eurostat, 2021). For countries where monthly deaths are not available, e.g., Tunisia, Israel, and Egypt, the monthly mean deaths averaged over all other countries in this region were used as proxy (Fig. A2). Total monthly deaths were then equally distributed to each day of the month. We denoted the daily number of deaths (baseline mortality) as $BM_d$.

An ERF associates the proportional increase in exposure of an air pollutant with the potential adverse health outcomes, typically expressed as relative risk (RR). The RR is a ratio of incidences (e.g., deaths) exposed to air pollution relative to incidences with no exposure. The RR can be estimated either by 1) pre-defined formulas or ranges of values from studies or meta-analyses, or 2) by integrated ERF approaches (Burnett et al., 2014; Cohen et al., 2017). Here, we chose the former approach, adopting RR values for short-term exposure mainly from a recently published systematic review by Orellano et al. (2020). To assess the uncertainty due to different RR estimates, we additionally calculated health impact estimates with RRs from different reviews published before (World Health Organization, 2013; Orellano et al., 2020; Vicedo-Cabrera et al., 2020; Liu et al., 2019). All of these RRs refer to risk of all-cause all-age mortality associated with short-term exposure to air pollutants, and thus no age groups are specified throughout this study. The RRs together with their respective 95% confidence intervals (CIs) are listed in Tab. 1.

https://doi.org/10.5194/nhess-2023-111
Preprint. Discussion started: 18 July 2023


Natural Hazards and Earth System Sciences
Discussions

| | Relative risk (95% CI) | |
|---|---|---|
| | $PM_{2.5}$ | $O_3$ |
| Orellano et al. (2020) | 1.0065 (1.0044–1.0086) | 1.0043 (1.0034–1.0052) |
| WHO (2013) | 1.0123 (1.0045-1.0201) | 1.0029 (1.0014-1.0043) |
| Liu et al. (2019)* | 1.0068 (1.0059-1.0077) | – |
| Vicedo-Cabrera et al. (2020) | – | 1.0018 (1.0012-1.0024) |

* 2-day moving average is used as the exposure metric instead of the daily mean used elsewhere.

**Table 1.** Relative risks ($RR_{\Delta 10}$) with 95% confidence interval (CI) of all-cause mortality associated with short-term exposure to $PM_{2.5}$ and $O_3$ for an increase of 10 $\mu$g/m$^3$ concentration, obtained from selected meta-analysis or multi-city studies published before.

Given a linear relationship and an increase of population exposure ($\Delta C$) of 10 $\mu$g/m$^3$, the RR is defined as

$$RR = e^{\beta \Delta C}. \tag{2}$$

From Eq. 2 we can back out the coefficient $\beta = \ln RR / \Delta C$ and use it to estimate RR for arbitrary $\Delta X$:

$$RR(\Delta X) = e^{\beta(\Delta X - X_0)}, \tag{3}$$

where $X_0$ is the theoretical minimum risk exposure level, below which no additional risk is assumed. In line with previous works (e.g., Graham et al., 2021; Macintyre et al., 2016), we assume $X_0$ to be zero. We then derived excess exposures to an air pollutant $i$ emitted from wildfires as the difference in population exposure between the fire and no-fire simulations for a country $J$:

$$\Delta Cp_{i,J} = Cp_{i,J}^{fire} - Cp_{i,J}^{no-fire} \tag{4}$$

To account for the health impacts on the population level, the population attributable fraction (PAF), defined as the fraction of adverse health outcomes in a population attributable to a specific exposure, is computed using the formula (Mansournia and Altman, 2018):

$$PAF = 1 - \frac{1}{RR} \tag{5}$$

The excess number of deaths attributable to wildfire-caused exposure to air pollutant $i$ for a country $J$ within the entire period of simulation ($E_{i,J}$) is computed as:

$$E_{i,J} = \sum_{d=1}^{N} (BM_{J,d} \times PAF_{i,J}), \tag{6}$$

where $BM_{J,d}$ is the baseline mortality (in number of deaths) of the country $J$ on day $d$ obtained before, and $N$ is the total number of simulation days.

https://doi.org/10.5194/nhess-2023-111
Preprint. Discussion started: 18 July 2023


Natural Hazards and Earth System Sciences
Discussions

#### 2.4.3 Estimate of uncertainty due to error propagation in excess mortality

Numerous sources of uncertainty exist for such a health impact assessment which have been discussed in details elsewhere (WHO, 2016). In this study, we accounted for the uncertainty arising from the multiplication of baseline mortality and relative risk, both of which are bounded with their respective 95% CIs. Assuming a normal distribution for both data sets ($x \sim \mathcal{N}(\mu, \sigma^2)$), the standard error (SE) of each data is derived as:

$$\mathrm{SE}(x) = (\mathrm{CI}^{\mathrm{upper}} - \mathrm{CI}^{\mathrm{lower}})/(2 \cdot z_{1-0.05/2}), \tag{7}$$

where $z_{1-0.05/2}$ is the 0.975 quantile of the standard normal distribution ($z_{0.975} \approx 1.96$). Then, the variance $\mathrm{Var}(x) = \mathrm{SE}(x)^2$. As PAF depends linearly on $1/RR$ (Eq. 5), its SE and variance are linear derivatives of those for $1/RR$.

To quantify the propagation of the uncertainties in the excess mortality estimates, two approaches were used. The first approach is based on the delta method (Ver Hoef, 2012). For the product of baseline mortality and PAF (as in Eq. 6), the joint standard error is calculated below:

$$\mathrm{SE}(\hat{x_1}\hat{x_2}) = \sqrt{\hat{x_1}^2\mathrm{Var}(\hat{x_2}) + \hat{x_2}^2\mathrm{Var}(\hat{x_1}) + 2\hat{x_1}\hat{x_2}\mathrm{Cov}(\hat{x_1}, \hat{x_2})}, \tag{8}$$

where $\hat{x_1}$ and $\hat{x_2}$ represent the expectations of baseline mortality and PAF, respectively. Since baseline mortality and PAF are mutually independent, their covariance $\mathrm{Cov}(\hat{x_1}, \hat{x_2})$ is zero. Equation 8 can be further shortened as:

$$\mathrm{SE}(\hat{x_1}\hat{x_2}) = \sqrt{\hat{x_1}^2\mathrm{Var}(\hat{x_2}) + \hat{x_2}^2\mathrm{Var}(\hat{x_1})} \tag{9}$$

The 95% confidence intervals for the product $x_1x_2$ are $\hat{x_1}\hat{x_2} \pm 1.96\mathrm{SE}(\hat{x_1}\hat{x_2})$.

The second approach is based on the Monte Carlo method. We respectively generated the normally distributed random samples of BM and PAF (with a sample size N = 1000) based on the expectations and SEs derived from Eq. 7. The 2.5% and 97.5% percentiles of the sample composed of the element-wise product of BM and PAF designated the lower and upper bounds of the 95% CIs for their product. Repeating for 100 times, the respective mean values of lower and upper bounds quantified the uncertainty for the estimated health impacts.

We used the R software (version 4.1.1) (R Core Team, 2021) and the *sf* package (version 1.0-4) (Pebesma, 2018) to perform the statistical and geo-spatial analyses.

## 3 Results

### 3.1 Model validation

Overall, WRF-Chem model performance is on par with recent multi-model inter-comparison studies of air quality models over Europe and North America (Im et al., 2015a, b) and produced accurate estimates for the concentrations of $PM_{2.5}$ and $O_3$ when compared to the AirBase dataset. Table B1 lists the model performance metrics for simulations of each air pollutant. The WRF-Chem model is prone to overestimate the concentration of air pollutants relative to the AirBase observations, except $PM_{2.5}$.

https://doi.org/10.5194/nhess-2023-111
Preprint. Discussion started: 18 July 2023


Natural Hazards and Earth System Sciences Discussions

Figures B1-B4 in Appendix B show normalized Taylor diagrams for WRF-Chem simulations of each air pollutant for rural, sub-urban, and urban AirBase stations. The estimates of $PM_{2.5}$ from the WRF-Chem simulations were marginally better for daily mean values than for hourly values when compared to the observations, whereas the performance exhibited no significant difference between stations of different types. The correlation coefficients between the simulated and observed concentrations (on polar axes) range from 0.4 to 0.7 (Fig. B1). By comparison, aggregating hourly observations of $O_3$ to daily means does not help increase the model performance. On the contrary, the model performance of reproducing the $O_3$ variation dropped with the mean IOA decreasing from 0.65 to 0.51 (Tab. B2). The type of station does not seem to affect the model performance in estimating $O_3$ concentration.

The stringent criteria on the data's status of verification have significantly reduced the number of AirBase stations available for model evaluation. The most stations remained for evaluation are located in a limited number of countries (e.g., Italy, Greece, and Bulgaria) and mostly in urban or suburban areas. We note that a perfect simulation, especially of urban stations cannot be expected due to the very different representativeness of station measurements and the 20 km horizontal resolution of WRF-Chem. Furthermore, the uneven spatial spread of stations and the over-representation of certain station type in the model evaluation could further worsen the performance metrics.

### 3.2 Spatio-temporal patterns of air pollutant concentrations

Figure 2a shows the spatial pattern of the WRF-Chem simulated $PM_{2.5}$ concentration as average over the entire period based on the fire scenario. The mean $PM_{2.5}$ concentrations range from 1 to 150 $\mu g/m^3$ across the region. High $PM_{2.5}$ loads are visible in regions that are already heavily polluted even in the absence of wildfires, e.g., in the Po Valley of Italy and the capital region of Serbia.

Figure 2b and c show the spatial pattern of fires-caused $PM_{2.5}$ concentration relative to that under no-fires scenario, and the percentage of $PM_{2.5}$ loads attributable to wildfires. The increased $PM_{2.5}$ concentrations caused by wildfires are mainly observed in the Balkans, Greece, and southern Italy, coinciding with the distribution of fire events within the simulation period (Fig. 1 b-c).

Diurnally, the $PM_{2.5}$ concentration is subject to the mixing layer height (Fig. C1). The daytime troughs reflect strong turbulent exchange and dilution within the mixed layer, whereas stable nighttime boundary layer enables $PM_{2.5}$ to accumulate (Manning et al., 2018).

Figure 3 shows the spatial pattern of WRF-Chem-simulated $O_3$ concentrations. In contrast to the $PM_{2.5}$ pattern, the $O_3$ concentration demonstrates an upward gradient from urban agglomerations to non-urban surroundings, indicating titration by large urban $NO_x$ emissions (Sillman, 1999).

The overall effect of the wildfires on $O_3$ is more widespread due to the longer atmospheric formation and lifetime of $O_3$, and is hence visible on a country level (Fig. C2). Interestingly, the border region between Bulgaria and Romania is observed to be one of regions most affected by wildfire-caused $O_3$ pollution, which may be accounted for by the location-specific topography and the fact that it is located downwind of a number of fires that occurred during the season. The region on the lower Danube

https://doi.org/10.5194/nhess-2023-111
Preprint. Discussion started: 18 July 2023


Natural Hazards and Earth System Sciences
Discussions

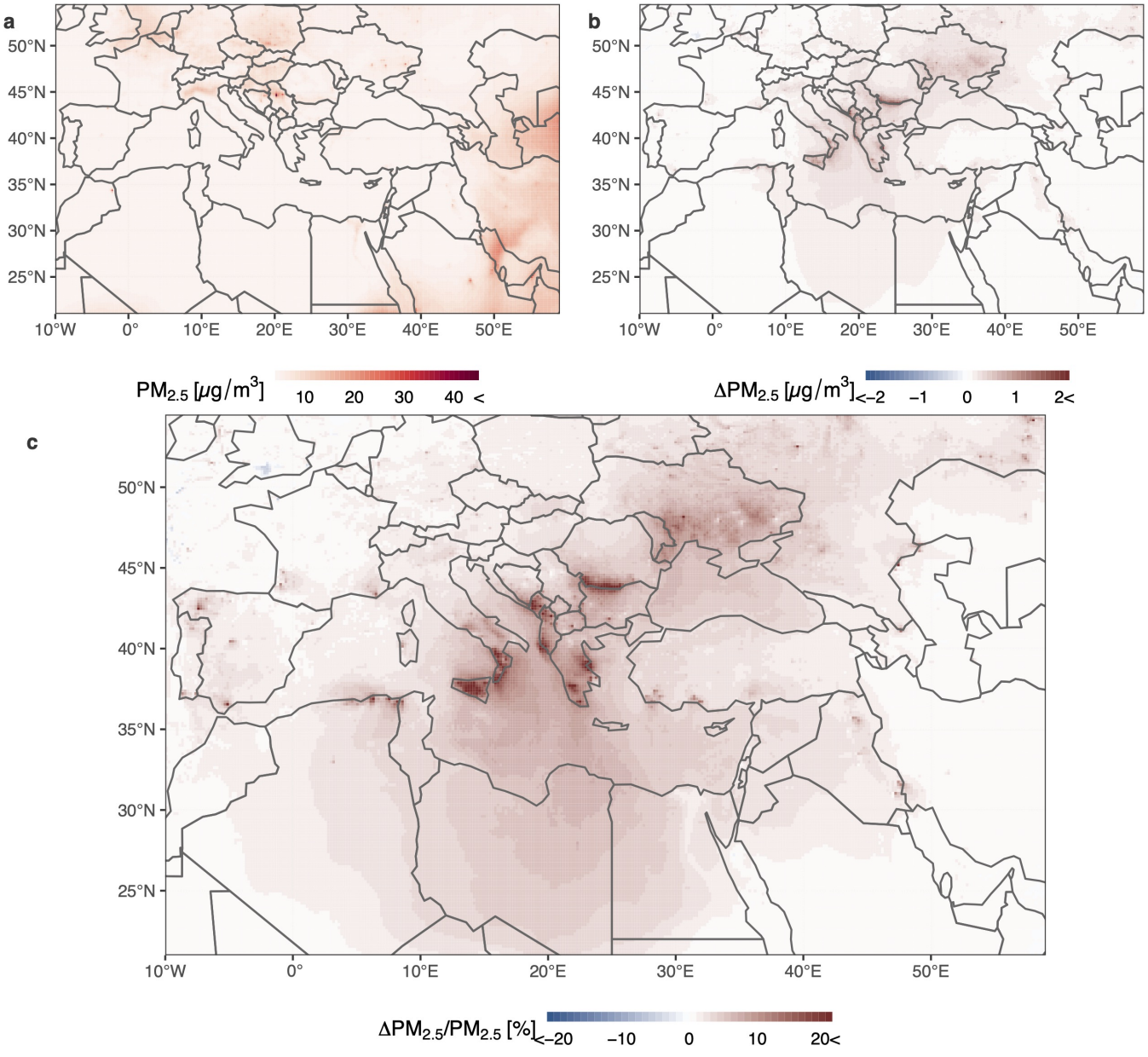


**Figure 2.** Spatial pattern of multi-month mean $PM_{2.5}$ concentrations simulated by WRF-Chem under the fires scenario and the difference relative to the no-fires scenario. a) $PM_{2.5}$ concentration simulated under fires scenario, b) $PM_{2.5}$ concentration under fires scenario relative to no-fires ($\Delta PM_{2.5} = PM_{2.5}^{fires} - PM_{2.5}^{no\text{-}fires}$), c) $PM_{2.5}$ concentration attributable to wildfires in percentages ($\Delta PM_{2.5}/PM_{2.5}^{fires}$). The increased $PM_{2.5}$ concentrations caused by wildfires are mainly observed in the Balkans, Greece, and southern Italy, whereas the regions with high background industrial pollution (hot spots in the panel a) show a slight decrease in ambient $PM_{2.5}$ concentration.

https://doi.org/10.5194/nhess-2023-111
Preprint. Discussion started: 18 July 2023


Natural Hazards and Earth System Sciences Discussions

plain is further bounded by the Carpathian Mountains to the North and West and by the Balkan Mountains to the South which forms a semi-closed topographical feature, channeling and concentrating air pollutants emitted from wildfires.

Figure C2 shows the diurnal pattern of $O_3$, which is determined by the presence of sunlight, as $O_3$ is formed primarily by photo-chemical reactions.

Figures C3 and C4 show the temporal pattern of $NO_2$ and $SO_2$ concentrations respectively, while their spatial patterns are shown in Fig. D1 and D2. The hot spots of $NO_2$ and $SO_2$ are principally found in cities, along artery roads and shipping routes, and in large point sources like power plants and oil and gas refineries (Fig. D2a). By comparison to $O_3$, increases of $NO_x$ and $SO_2$ are less visible on a country level (Fig. C3 and C4), as their effects are limited locally due to their relatively shorter atmospheric lifetime, and the dilution into comparatively high pre-existing background concentrations. Similar to $PM_{2.5}$, the diurnal pattern of $NO_2$ and $SO_2$ concentration is determined by the mixing layer height. Meanwhile, we found the expected increases in the concentration of OH in the fire simulation (Fig. D3), which will lead to additional formation of secondary PM.

### 3.3 Population-weighted exposure to major air pollutants

Figure 4 depicts the multi-month mean population-weighted exposures to four air pollutants under fires (red dots), and no-fires (blue dots) scenarios. For the time series of population-weighted exposures to air pollutants in individual countries, please refer to Figs. E1-E4. Countries in Balkans (e.g., Albania, Serbia, North Macedonia, Montenegro, and Bulgaria), Romania, and Greece are among the most affected regions by the wildfire-caused $PM_{2.5}$ and $O_3$ pollution, in line with the incidence of wildfires within the simulation period. By contrast, wildfires have not resulted in a discernible increase of population exposure to $NO_2$ and $SO_2$ within the simulation period and region. Therefore, we estimate the wildfire-associated health impacts based primarily on $PM_{2.5}$ and $O_3$ exposures.

### 3.4 Wildfire-caused excess mortality

Figure 5 a-b shows the excess number of deaths for each country estimated based separately on RRs of short-term exposure to $PM_{2.5}$ and $O_3$ obtained from the meta-analysis by Orellano et al. (2020). The 95% CIs are estimated using the Monte Carlo method described in Section 2.4.3. The exact number of deaths for each country and the entire region are available in Tab. A2.

Countries with a large population such as Italy and Egypt are estimated to have higher excess deaths due to short-term exposure to wildfire-caused $PM_{2.5}$ and $O_3$. Although wildfires are not frequently observed in Egypt (Fig. 1 b), the deaths estimated are significant and can be attributed to the transport of air pollution caused by wildfires occurring elsewhere in the Mediterranean basin, clearly indicating the widespread impact of wildfires on the whole Mediterranean basin.

Figure 5c-d sum up the excess deaths attributable to short-term exposure to $PM_{2.5}$ and $O_3$ in the entire region of investigation during mid-July to early October, 2021, based on RRs suggested by different publications. Based on the RR values from Orellano et al. (2020), there are 87 (95% CI: 56-118) deaths attributable to the short-term exposure to wildfire-caused $PM_{2.5}$. This estimate is close to the one based on Liu et al. (2019) – 90 (95% CI: 73-108). In comparison, 164 (95% CI: 57-270) excess deaths are estimated based on the RRs from World Health Organization (2013), albeit with a pronounced range of uncertainty.

https://doi.org/10.5194/nhess-2023-111
Preprint. Discussion started: 18 July 2023


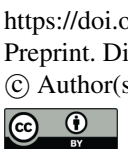

Natural Hazards and Earth System Sciences
Discussions
Open Access
EGU

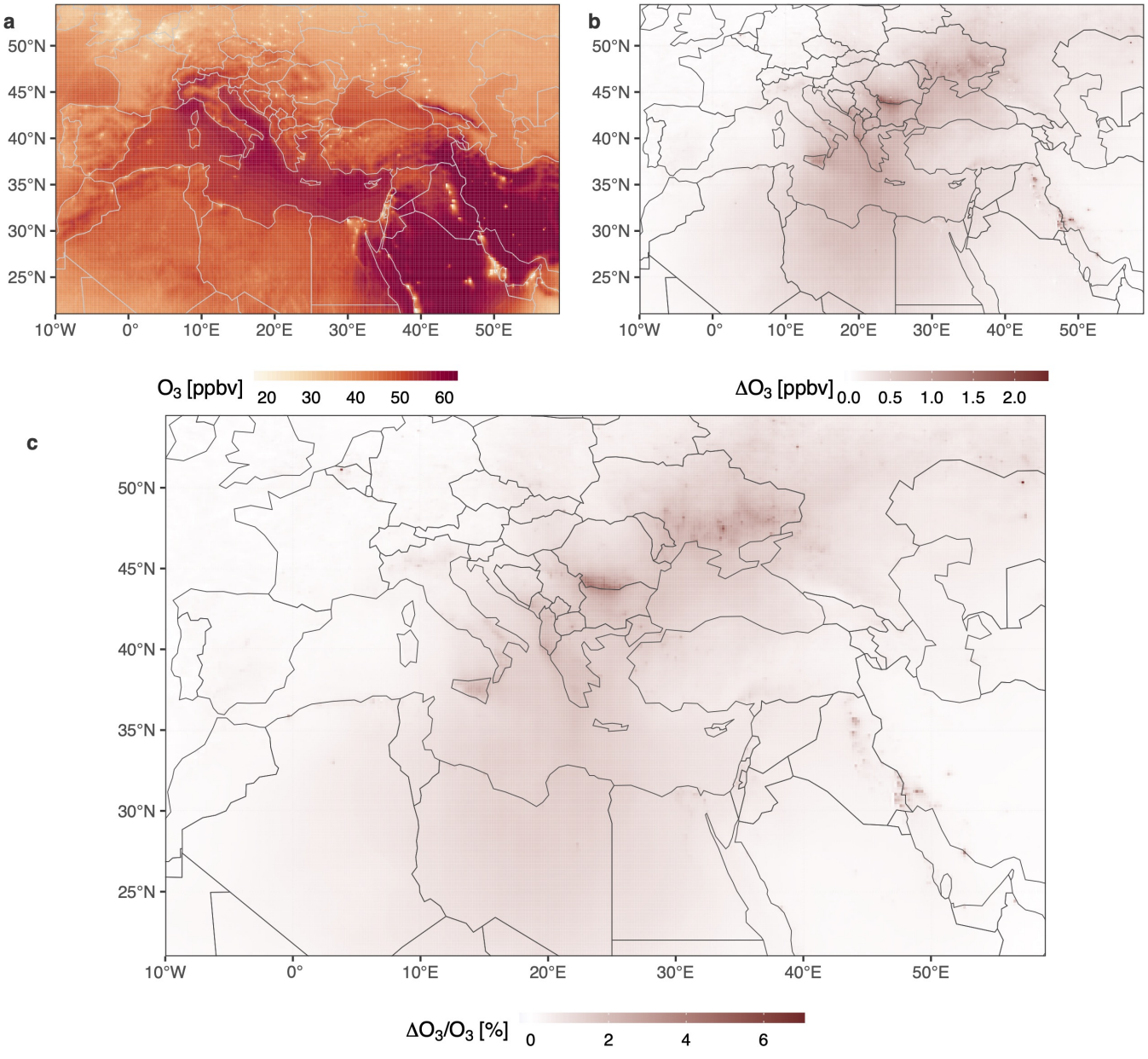


**Figure 3.** Spatial pattern of multi-month mean $O_3$ concentrations simulated by WRF-Chem under the fires scenario and the difference relative to the no-fires scenario. a) $O_3$ concentration simulated under fires scenario, b) $O_3$ concentration under fires scenario relative to no-fires ($\Delta O_3 = O_3^{fires} - O_3^{no\text{-}fires}$), c) $O_3$ concentration attributable to wildfires in percentages ($\Delta O_3/O_3^{fires}$).

https://doi.org/10.5194/nhess-2023-111
Preprint. Discussion started: 18 July 2023


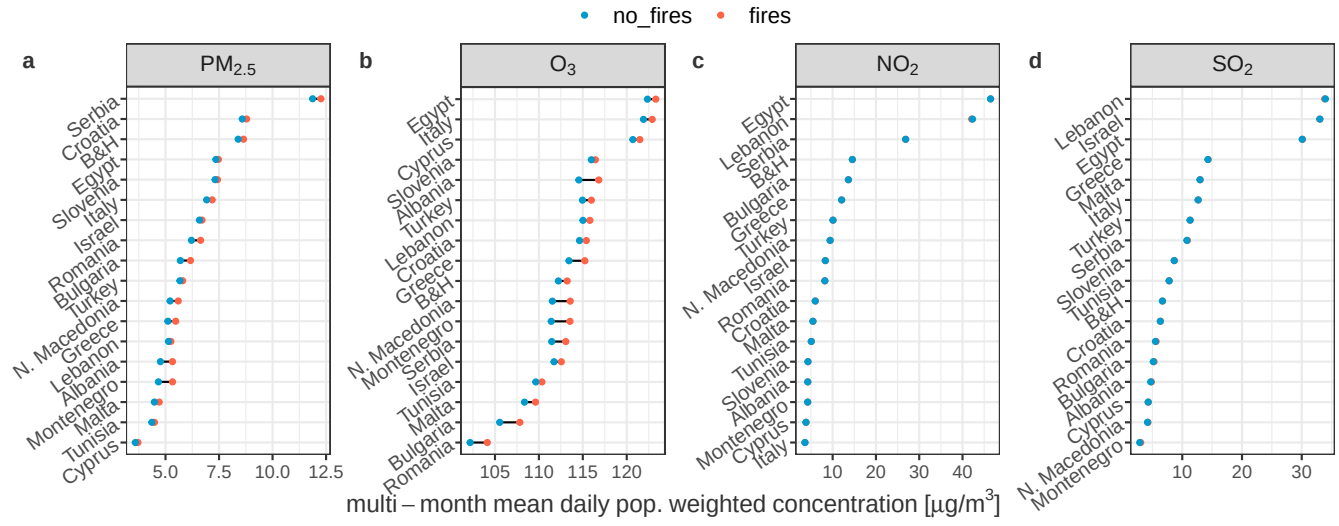


**Figure 4.** Multi-month daily mean population weighted concentration of air pollutants, fires scenario versus no-fires scenario. For pollutants other than $O_3$, the daily mean concentration is used, while the daily mean 8-h average (DMA8) for $O_3$. B&H stands for Bosnia and Herzegovina.

With regard to the excess deaths attributable to short-term $O_3$ exposure, 289 (95% CI: 214 - 364]) excess deaths are estimated based on Orellano et al. (2020), remarkably exceeding the estimates based on World Health Organization (2013) (195, 95% CI: 93 - 297) and Vicedo-Cabrera et al. (2020) (121, 95% CI: 77 - 166).

## 4 Discussion

In general, we found larger health impacts due to wildfire-associated exposure to $O_3$ than to $PM_{2.5}$. As the relative risk of exposure to $O_3$ is actually lower than that of $PM_{2.5}$ exposure (Tab. 1), the reason for this surprising finding is shown to be attributable to the more widespread impact of wildfires on $O_3$ due to a longer overall atmospheric lifetime of $O_3$ (about a month) in contrast to $PM_{2.5}$ (days to weeks) (Task Force on Hemispheric Transport of Air Pollution (TF HTAP), 2010; Liang et al., 2018).

We refrained from deciding whether the excess deaths attributed to each pollutant can simply be added up to generate a synthesized estimate of health impacts as a result of the simultaneous exposure to multiple pollutants. The solution to this problem demands a thorough knowledge of correlations between health impacts of each pollutant (World Health Organization, 2013), and analysis of their confounding effects (Anderson et al., 2012; Bell et al., 2007). Although several statistical methods have been proposed to address the multi-collinearity issues in concurrent exposure (Stafoggia et al., 2017; Wei et al., 2020), they have not been widely adopted, including in studies that underlay the systematic reviews by Orellano et al. (2020); World Health Organization (2013). Therefore, results based on these reviews should be interpreted with caution, as confounders were

https://doi.org/10.5194/nhess-2023-111
Preprint. Discussion started: 18 July 2023


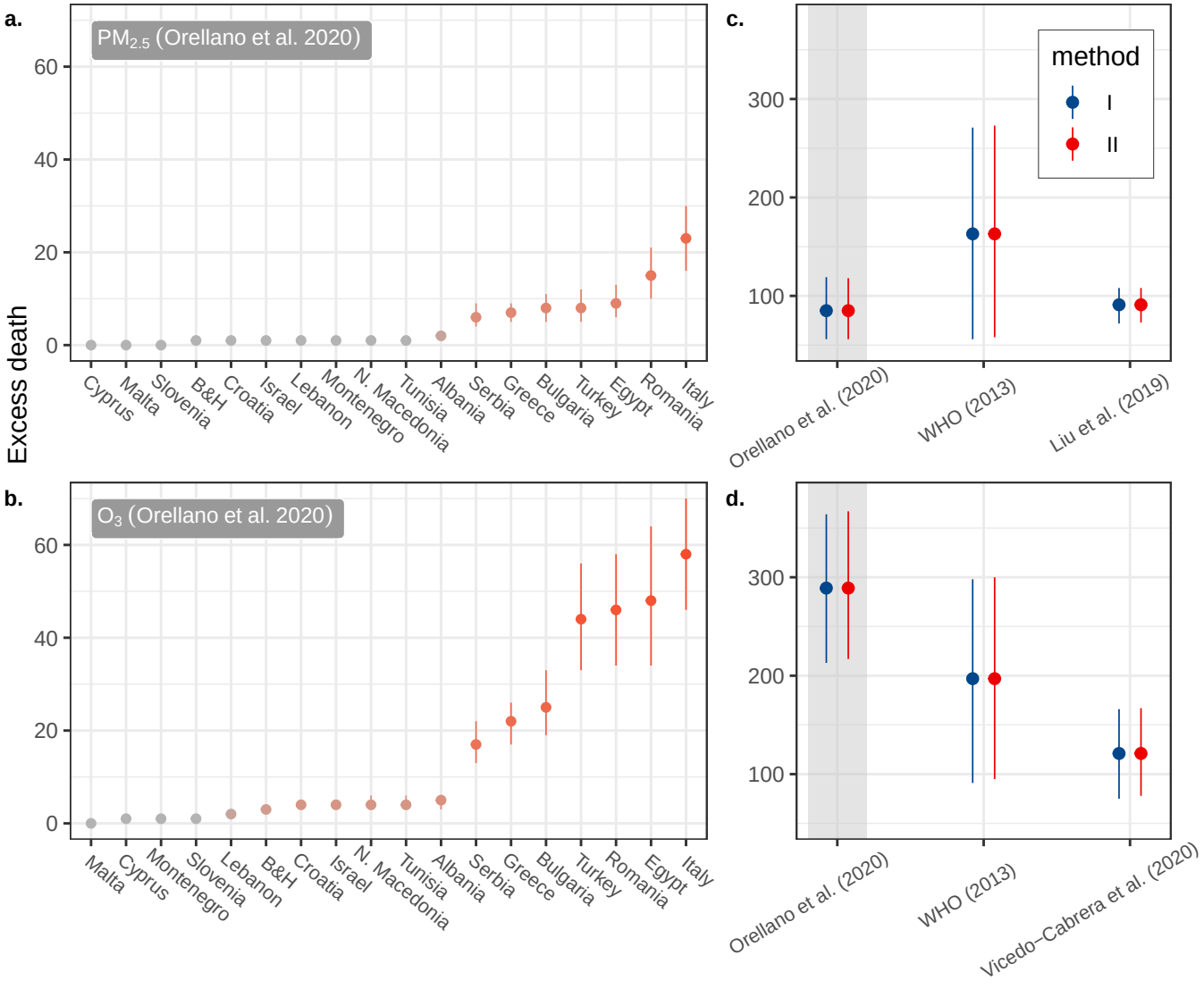


**Figure 5.** Excess deaths with uncertainties estimated based on relative risks of short-term exposure to $PM_{2.5}$ and $O_3$. a-b) wildfire-caused excess deaths with 95% CIs for each country included in the study based on relative risk values for short-term $PM_{2.5}$ and $O_3$ exposures from Orellano et al. (2020). c) Total excess deaths estimated using relative risk values from different meta-analyses (with the vertical gray band indicating the ones used in panels a and b), based on short-term exposure to $PM_{2.5}$ and $O_3$, respectively. The 95% CIs were estimated using the Delta (I) and Monte Carlo (II) methods. In Liu et al. (2019), the 2-day moving average of daily mean $PM_{2.5}$ concentrations was used to estimate the excess mortality.

https://doi.org/10.5194/nhess-2023-111
Preprint. Discussion started: 18 July 2023


Natural Hazards and Earth System Sciences
Discussions

not adequately adjusted for. As a result, it remains inconclusive whether to sum up the death estimates based on different air pollutants. All the aforementioned aspects can substantially affect the outcomes of the health impact assessment, making it difficult to narrow down the range of real health impacts attributable to wildfire-caused air pollution beyond what we have shown here.

The WRF-Chem model enables a temporally and spatially resolved exposure estimate, while accounting for primary emissions from wildfires and subsequent secondary chemical and physical processes. To date, the health impact assessment of air pollution is limited to a subset of its proxies (e.g., $PM_{2.5}$, $NO_2$, $O_3$), with their exposures being measured by mass. This simplification is increasingly challenged by mounting evidence that the toxicity of air pollution depends to a large extent on the chemical composition and atmospheric ageing rather than the mass itself. Especially, several studies point to the fact that PM arising from wildfires is more toxic to lungs compared with PM from normal ambient air (Wegesser et al., 2009; Dong et al., 2017; Xu et al., 2020). In the future, the ability of such modeling systems to estimate further harmful trace gases as well as chemically-speciated PM may help overcome such limitations, leading to better association and causation in epidemiological analysis.

We have accounted for uncertainties arose from the baseline mortality data and ERFs. However, we have to acknowledge several sources of uncertainty that have not been taken into account within this study. The health impacts estimated within the study is limited to the excess mortality due to short-term exposure to air pollution aggravated by wildfires. This does not take into account direct loss of life and hospital admissions caused by the direct exposure to radiant heat/smoke/flames of wildfires, nor the consequent impairment of life quality.

Though broadly validated, the WRF-Chem model results contain a certain degree of uncertainty in exposure estimation. The uncertainty could originate from the model configuration (e.g., the horizontal and vertical grid setting of simulation domain, and parameterization schemes adopted to account for the atmospheric physics and chemistry), model inputs (e.g., boundary meteorology, and inventories on anthropogenic and fires-associated emissions), as well as the representation of particles and their size distribution within the model (Im et al., 2018).

The horizontal resolution of 20 km set in the WRF-Chem simulation may be too coarse to represent urban areas and their related impacts on the dispersion and transformation of air pollutants sourced from wildfires. This may lead to an underestimation of particular matter and an overestimation of $O_3$ in urban areas (Im et al., 2015a). Due to its complex nature, the model-associated uncertainty has not been addressed in the study. However, this can be the focus of future research.

A further source of uncertainty lies in the ERFs adopted for the health impact assessment. Although ERFs derived from meta-analysis are thought to deliver less biased and impartial evidence on the association between exposure and health outcomes, they are prone to several other biases, e.g., publication bias and language bias, which may distort the evidence (Page et al., 2021). Meanwhile, current ERFs are based primarily on exposures measured in urban or suburban settings, making the exposure estimate for rural areas more prone to misclassification errors. Even though rural areas normally exhibit a lower level of PM and are thought to be less polluted, the rural air can demonstrate similar levels of cellular oxidative potential as in cities, due largely to more toxic chemicals emitted from agriculture activities (Wang et al., 2022). On the other hand, neither measurements by

https://doi.org/10.5194/nhess-2023-111
Preprint. Discussion started: 18 July 2023


monitoring networks nor model simulations, are able to reproduce the individual exposure which is subject to a variety of factors such as personal behavior, socioeconomic status, and preexisting health conditions (Evangelopoulos et al., 2020).

Subject to the RR value used, the estimated health burdens in association with short-term $O_3$ exposure differ markedly. The RR value suggested by Orellano et al. (2020) was attained through a systematic review based on the most recent studies, serving as an update of the previous report by World Health Organization (2013). In comparison, Vicedo-Cabrera et al. (2020) suggested a considerably lower RR for short-term exposure to $O_3$, resulting in a smaller estimate of excess deaths. As both studies differ in methodology and underlying database leading to the RRs, the reason for the discrepancy remains unexplored and is beyond the scope of this study.

In all estimates, the choice of methods for quantifying the uncertainty of excess deaths exhibits a minor impact on the results. The Delta method, compared with the Monte Carlo method, is prone to slightly underestimate the lower and upper bounds of the 95% CI.

We excluded the health impact assessment based on short-term exposure to $PM_{10}$, another widely used proxy indicator for air pollution, to avoid double counting of the PM-associated health effects. This is based on the fact that $PM_{2.5}$ accounts for an overwhelming proportion of PM-associated health effects (Lu et al., 2015; Liu et al., 2019).

## 5 Conclusions

We have assessed the health impacts due to the short-term exposure to air pollution caused by wildfires over the eastern and central Mediterranean basin in the summer 2021. The exposures were estimated using a fully coupled atmospheric chemistry model under fire and no-fire scenarios, respectively, while the consequent health impacts were quantified based on well-established ERFs from selected systematic reviews. We estimated that the 2021 summer wildfires result in an excess number of deaths ranging from approximately 87 (95% CI: 56-118) to 289 (95% CI: 214 - 364]), depending on the targeted pollutants which population are exposed to, and on their respective ERFs. Future work is needed to reduce the uncertainties resulted from estimates of both exposures and health effects, while simultaneously augmenting the computational performance of the methodology used. To this end, it is worth further exploring the ensemble or hybrid approaches which combine both physically based atmospheric chemistry transport models and computationally efficient statistical models (Im et al., 2018; Conibear et al., 2021; Di et al., 2019; Shtein et al., 2019; Hough et al., 2021).

https://doi.org/10.5194/nhess-2023-111
Preprint. Discussion started: 18 July 2023


Natural Hazards and Earth System Sciences
Discussions

## Appendix A: Population and mortality data

**Table A1.** Countries included in the study and their respective population in 2020, obtained from the World Bank's World Development Indicators database (World Bank, 2020).

| | name | ISO-2 | ISO-3 | pop. (in Mio.) |
|---|---|---|---|---|
| 1 | Albania | AL | ALB | 2.84 |
| 2 | Bosnia and Herzegovina (B&H) | BA | BIH | 3.28 |
| 3 | Bulgaria | BG | BGR | 6.93 |
| 4 | Cyprus | CY | CYP | 1.21 |
| 5 | Egypt | EG | EGY | 102.33 |
| 6 | Greece | GR | GRC | 10.72 |
| 7 | Croatia | HR | HRV | 4.05 |
| 8 | Israel | IL | ISR | 9.22 |
| 9 | Italy | IT | ITA | 59.55 |
| 10 | Lebanon | LB | LBN | 6.83 |
| 11 | Montenegro | ME | MNE | 0.62 |
| 12 | North Macedonia (N. Macedonia) | MK | MKD | 2.07 |
| 13 | Malta | MT | MLT | 0.53 |
| 14 | Romania | RO | ROU | 19.29 |
| 15 | Serbia | RS | SRB | 6.91 |
| 16 | Slovenia | SI | SVN | 2.10 |
| 17 | Tunisia | TN | TUN | 11.82 |
| 18 | Turkey | TR | TUR | 84.34 |
| | SUM | | | 334.62 |

https://doi.org/10.5194/nhess-2023-111
Preprint. Discussion started: 18 July 2023


Natural Hazards and Earth System Sciences
Discussions

**Table A2.** Excess number of deaths for individual countries and the entire region estimated based on wildfires-caused $PM_{2.5}$ and $O_3$ loads within the simulation period, with 95% confidence intervals (CIs) in brackets. The methods I and II refer to the Delta and Monte Carlo methods for the uncertainty estimation, respectively, which are described in details in Section 2.4.3 in the main text. The Delta method slightly underestimate the excess deaths compared to the Monte Carlo method. However, the difference is not significant.

| | **$PM_{2.5}$** | | **$O_3$** | |
|---|---|---|---|---|
| Country | Method I | Method II | Method I | Method II |
| Albania | 2 [1,2] | 2 [1,2] | 5 [3,6] | 5 [3,6] |
| B&H | 1 [1,2] | 1 [1,2] | 3 [2,4] | 3 [2,4] |
| Bulgaria | 8 [5,11] | 8 [5,11] | 25 [18,32] | 25 [19,33] |
| Croatia | 1 [1,2] | 1 [1,2] | 4 [3,5] | 4 [3,5] |
| Cyprus | 0 [0,0] | 0 [0,0] | 1 [0,1] | 1 [0,1] |
| Egypt | 9 [6,13] | 9 [6,13] | 48 [33,63] | 48 [34,64] |
| Greece | 7 [5,9] | 7 [5,9] | 22 [17,26] | 22 [17,26] |
| Israel | 1 [0,1] | 1 [0,1] | 4 [3,4] | 4 [3,4] |
| Italy | 23 [16,31] | 23 [16,30] | 58 [46,70] | 58 [46,70] |
| Lebanon | 1 [0,1] | 1 [0,1] | 2 [2,3] | 2 [2,3] |
| Malta | 0 [0,0] | 0 [0,0] | 0 [0,0] | 0 [0,0] |
| Montenegro | 1 [0,1] | 1 [0,1] | 1 [1,2] | 1 [1,2] |
| N. Macedonia | 1 [1,2] | 1 [1,2] | 4 [3,6] | 4 [3,6] |
| Romania | 15 [10,21] | 15 [10,21] | 46 [34,57] | 46 [34,58] |
| Serbia | 6 [4,9] | 6 [4,9] | 17 [12,22] | 17 [13,22] |
| Slovenia | 0 [0,0] | 0 [0,0] | 1 [1,1] | 1 [1,1] |
| Tunisia | 1 [1,2] | 1 [1,2] | 4 [3,6] | 4 [3,6] |
| Turkey | 8 [5,12] | 8 [5,12] | 44 [32,56] | 44 [33,56] |
| SUM | 87 [56,118] | 87 [57,118] | 289 [214,364] | 289 [218,366] |

https://doi.org/10.5194/nhess-2023-111
Preprint. Discussion started: 18 July 2023


Natural Hazards and Earth System Sciences
Discussions
Open Access
EGU

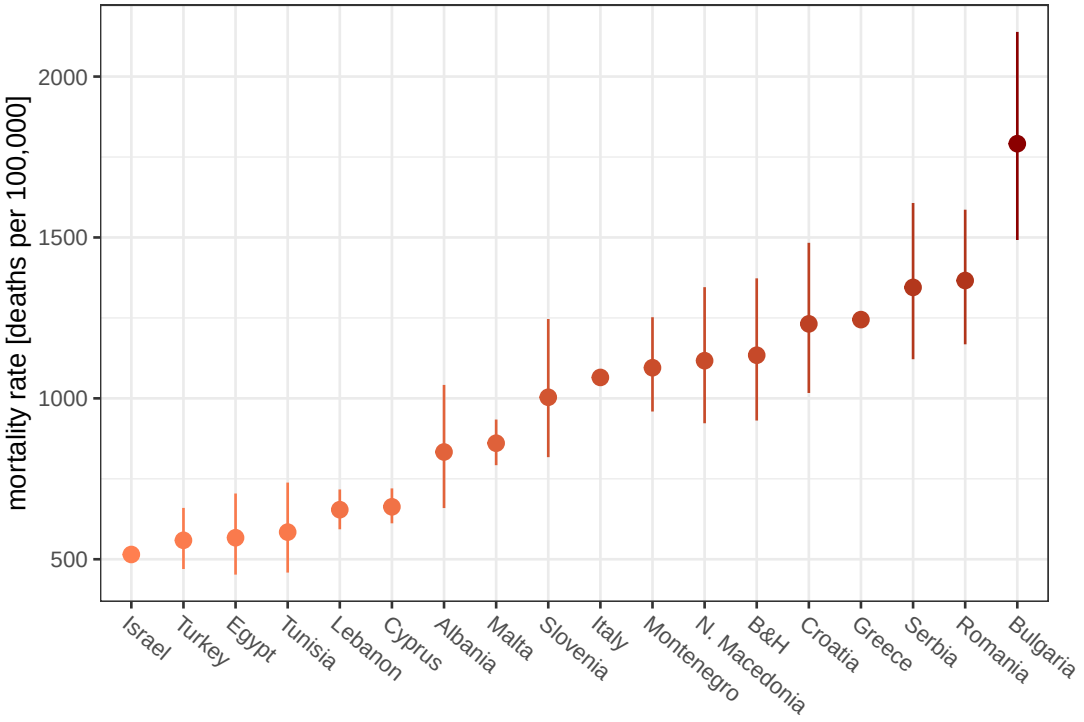


**Figure A1.** Baseline all-cause mortality in both genders 2019 for each country with 95% confidence intervals, downloaded from the Global Health Data Exchange Global Burden of Disease Collaborative Network (2020).The annual mortality rates of countries range from 515 (Israel) to 1791 (Bulgaria) deaths per 100,000 population. B&H stands for Bosnia and Herzegovina.

https://doi.org/10.5194/nhess-2023-111
Preprint. Discussion started: 18 July 2023


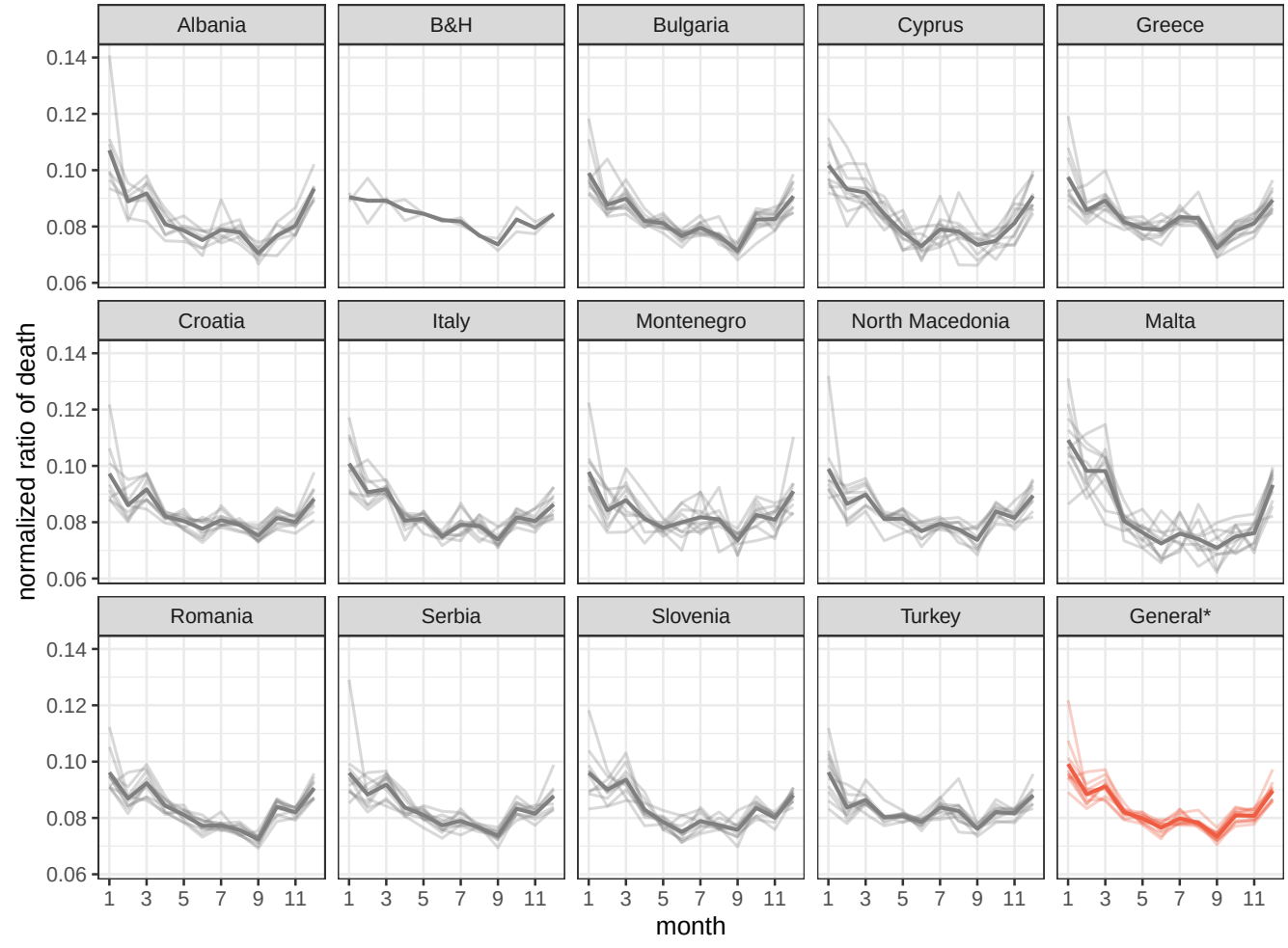


**Figure A2.** Multi-annual monthly mean normalized ratio of death averaged across 2010-2020 (dark gray, bold), underlaid with data for individual years (light gray) downloaded from Eurostat (2021). For countries where monthly death data are not available (e.g., Egypt, Israel, Lebanon), the monthly mortality is calculated based on the regional mean value averaged across all other countries (General*).

https://doi.org/10.5194/nhess-2023-111
Preprint. Discussion started: 18 July 2023


Natural Hazards and Earth System Sciences
Discussions

## Appendix B: Model performance of WRF-Chem

**Table B1.** Performance metrics used in this study for model evaluation. $N$ is the number of observations. $M_i$ and $O_i$ are modelled and observed values, respectively, while the overline indicates the arithmetic mean. $\sigma$ represents the standard deviation. Normalized standard deviation and correlation coefficient (Pearson's) are presented in a Taylor diagram (Figs. B1-B4). The index of agreement (IOA) is a standardized measure of the degree of model prediction error with a range between 0 and 1 (Willmott, 1981). A value of 1 indicates a perfect match, while 0 the worst.

| Metric | Expression | Range |
|---|---|---|
| Mean Bias (MB) | $\frac{1}{N}\sum_{i=1}^{N}(M_i - O_i)$ | $(-\infty, +\infty)$ |
| Normalized Mean Bias (NMB) | $\sum_{i=1}^{N}(M_i - O_i)/\sum_{i=1}^{N} O_i$ | $(-\infty, +\infty)$ |
| Normalized standard deviation | $\sigma_M/\sigma_O$ | $[0, +\infty)$ |
| Root mean square error (RMSE) | $\sqrt{\frac{1}{N}\sum_{i=1}^{N}(M_i - O_i)^2}$ | $[0,+\infty)$ |
| Correlation coefficient ($\rho$) | $\sum_{i=1}^{N}(M_i - \bar{M})(O_i - \bar{O})/(\sigma_M\sigma_O)$ | [0,1] |
| centred RMSE | $\sqrt{\sigma_M^2 + \sigma_O^2 - 2\sigma_M\sigma_O\rho}$ | $[0, +\infty)$ |
| Index of agreement (IOA) | $1 - \frac{\sum_{i=1}^{N}(M_i - O_i)^2}{\sum_{i=1}^{N}(\lvert M_i - \bar{O}\rvert + \lvert O_i - \bar{O}\rvert)^2}$ | [0, 1] |

https://doi.org/10.5194/nhess-2023-111
Preprint. Discussion started: 18 July 2023


Natural Hazards and Earth System Sciences
Discussions

**Table B2.** Performance metrics of the WRF-Chem for simulating daily and hourly mean concentrations of individual air pollutants from AirBase stations. Metrics shown are mean value of mean bias (MB), normalized mean bias (NMB), root mean square error (RMSE), and index of agreement (IOA), with their standard deviations in parentheses. Based on IOA, the model performs relatively well to reproduce the variations of $PM_{2.5}$ and $O_3$. It has a mediocre performance for $NO_2$, while it scores lowest in estimating $SO_2$. The model shows a generally positive bias relative to the AirBase observations for most air pollutants considered here except $PM_{2.5}$. The model underestimates $PM_{2.5}$ while overestimating $O_3$. The bias for $NO_2$, albeit small, fluctuates considerably among stations, and the same fluctuations are observed for $SO_2$. The particularly problematic simulations for $SO_2$ may be ascribed to the model configuration that the point source emissions of $SO_2$ (e.g., from power plants and industrial sites) are assigned directly to the immediate surface, leading a considerable overestimation of the surface ambient concentration.

| | | MB [$\mu g/m^3$] | NMB | RMSE [$\mu g/m^3$] | IOA |
|---|---|---|---|---|---|
| $PM_{2.5}$ | day | -4.60 (2.97) | -0.39 (0.20) | 6.45 (2.45) | 0.57 (0.10) |
| | hour | -6.54 (3.20) | -0.50 (0.19) | 9.21 (3.36) | 0.50 (0.09) |
| $O_3$ | day | 25.74 (19.18) | 0.45 (0.39) | 32.29 (12.99) | 0.51 (0.16) |
| | hour | 25.79 (19.21) | 0.46 (0.39) | 38.06 (11.74) | 0.65 (0.13) |
| $NO_2$ | day | 2.32 (7.41) | 0.29 (0.61) | 7.55 (5.12) | 0.52 (0.15) |
| | hour | -0.48 (9.96) | 0.13 (0.50) | 13.93 (10.43) | 0.47 (0.13) |
| $SO_2$ | day | 8.70 (20.17) | 0.88 (1.75) | 13.40 (19.54) | 0.40 (0.15) |
| | hour | 5.49 (19.77) | 0.38 (1.47) | 15.26 (25.44) | 0.36 (0.10) |

https://doi.org/10.5194/nhess-2023-111
Preprint. Discussion started: 18 July 2023


Natural Hazards and Earth System Sciences
Discussions

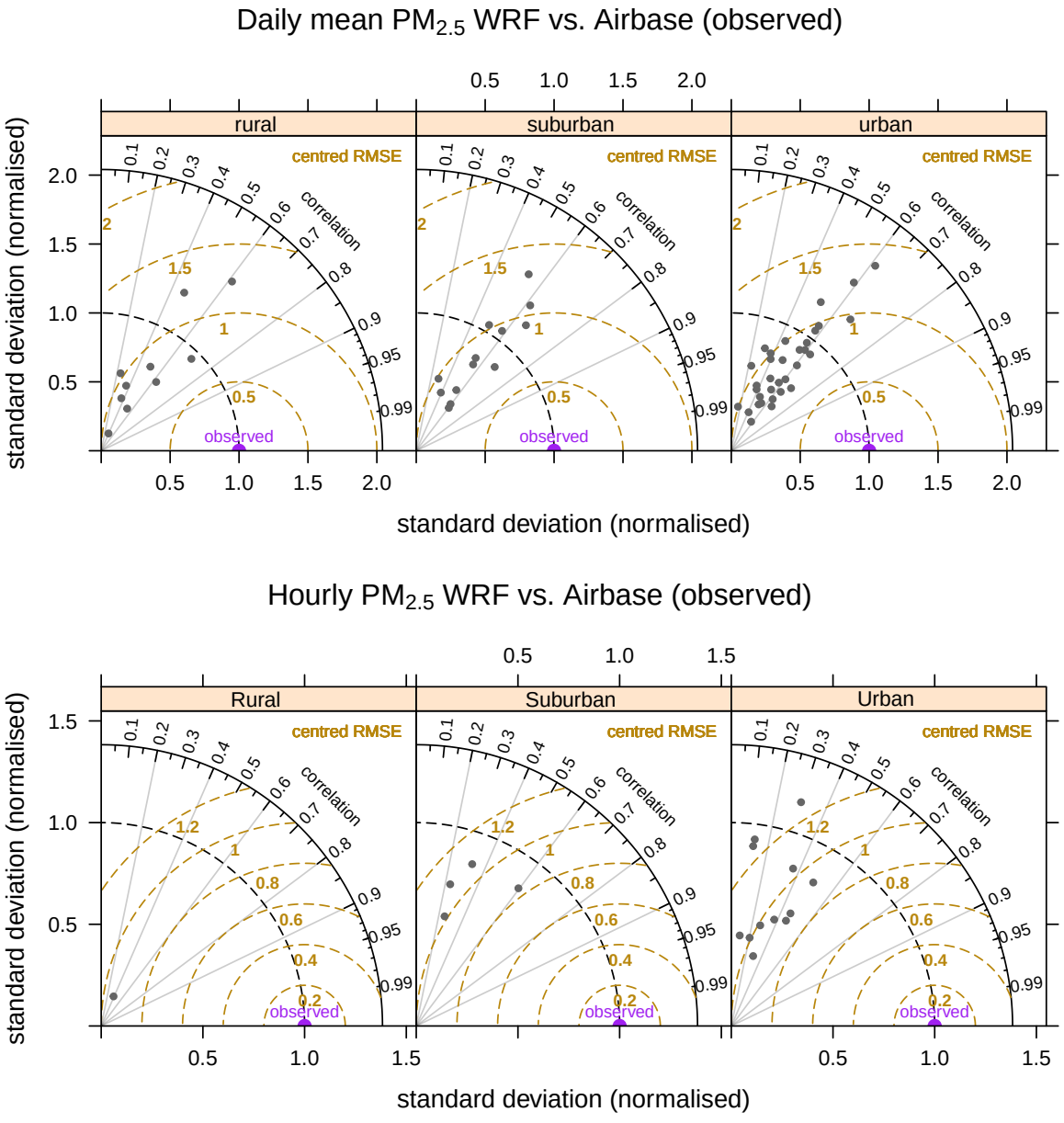


**Figure B1.** Evaluation of $PM_{2.5}$ concentration simulated by WRF-Chem using AirBase E1a & E2a air quality data. We only used the verified AirBase data with "verification code" equal to 1 (verified) or 2 (preliminary verified) in the metadata, and data from stations where more than 75% of observations are present during the entire period. Each AirBase station is spatially matched to a WRF grid cell (20 km). The hourly WRF values are also averaged to daily means for comparison with AirBase data from stations where only daily means were recorded. The model achieved a correlation coefficient of larger than 0.5 and centred RMSE below 1.0 for most stations in simulating daily mean $PM_{2.5}$. It slightly outperformed the model for reproducing the hourly mean $PM_{2.5}$.

https://doi.org/10.5194/nhess-2023-111
Preprint. Discussion started: 18 July 2023


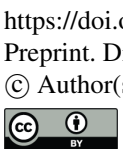

Natural Hazards and Earth System Sciences
Discussions
Open Access
EGU

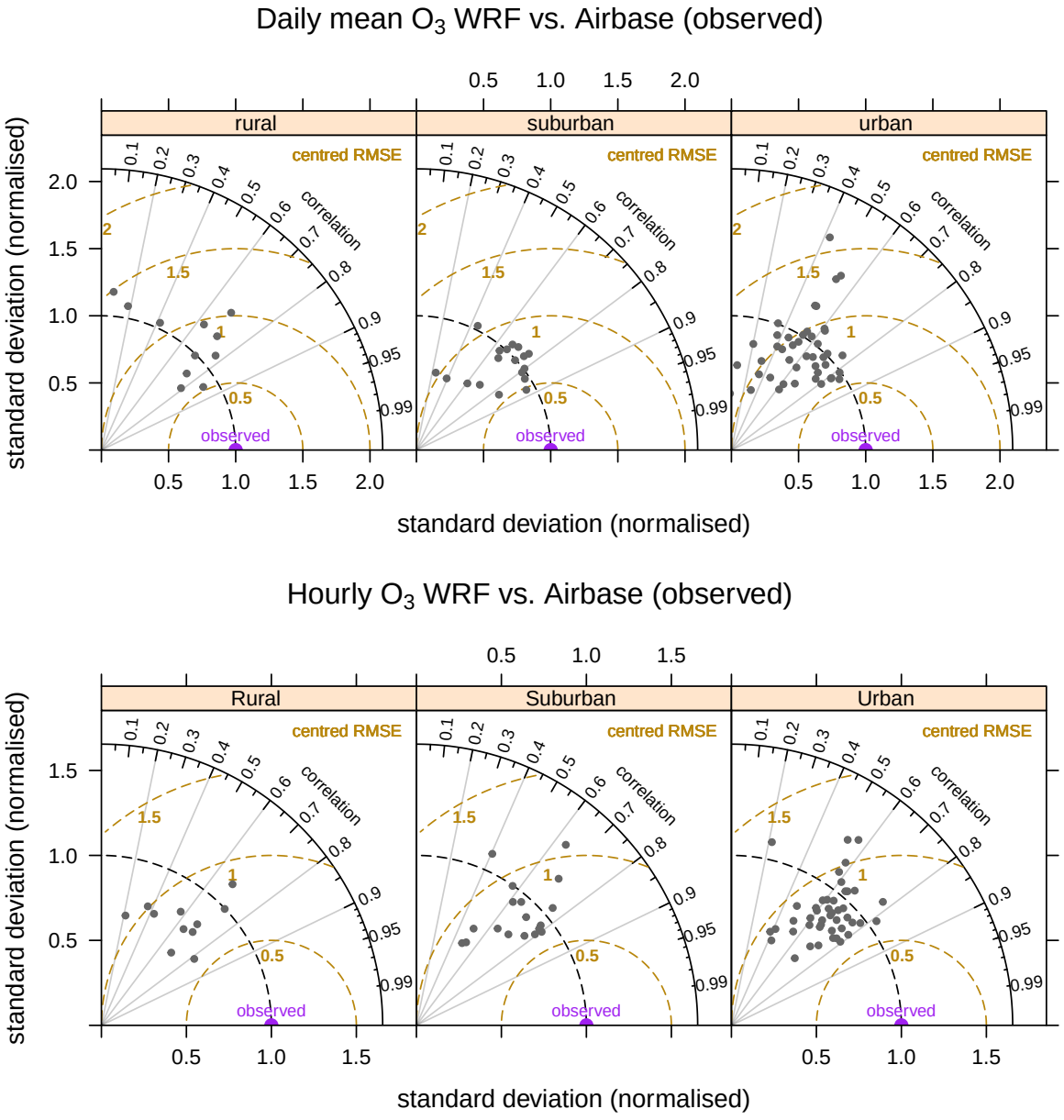


**Figure B2.** Evaluation of $O_3$ concentration simulated by WRF-Chem using AirBase data. The AirBase observations of $O_3$ are collected hourly. Aggregating hourly values to daily aggregates does not help increase the model performance. On the contrary, the model performance of reproducing the $O_3$ variation drops slightly with the mean IOA decreasing from 0.65 to 0.51.

https://doi.org/10.5194/nhess-2023-111
Preprint. Discussion started: 18 July 2023


Natural Hazards and Earth System Sciences
Discussions

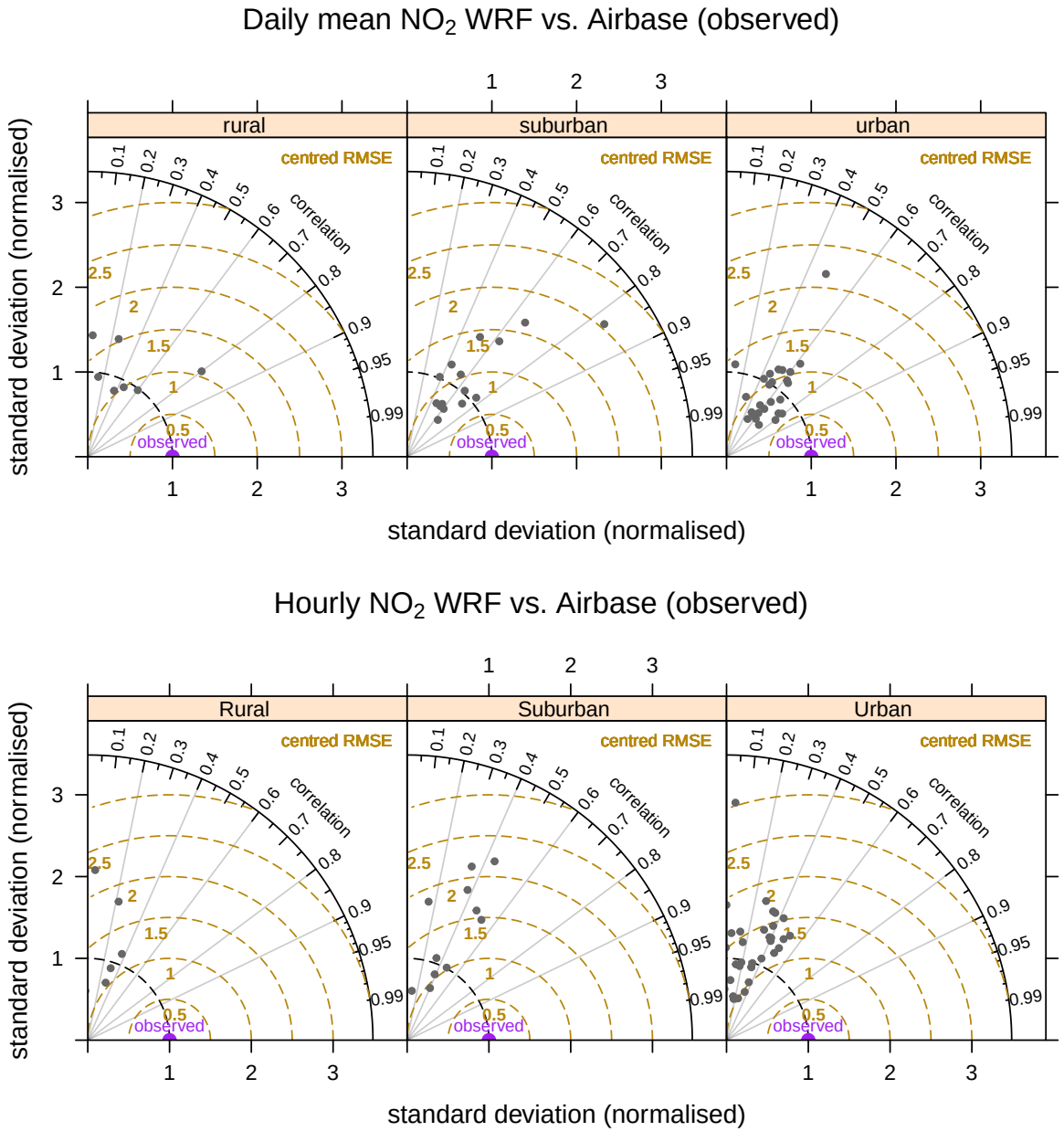


**Figure B3.** Evaluation of $NO_2$ concentration simulated by WRF-Chem using AirBase data. The model demonstrated a mediocre performance in simulating both daily and hourly mean of $NO_2$.

https://doi.org/10.5194/nhess-2023-111
Preprint. Discussion started: 18 July 2023


Natural Hazards and Earth System Sciences
Discussions

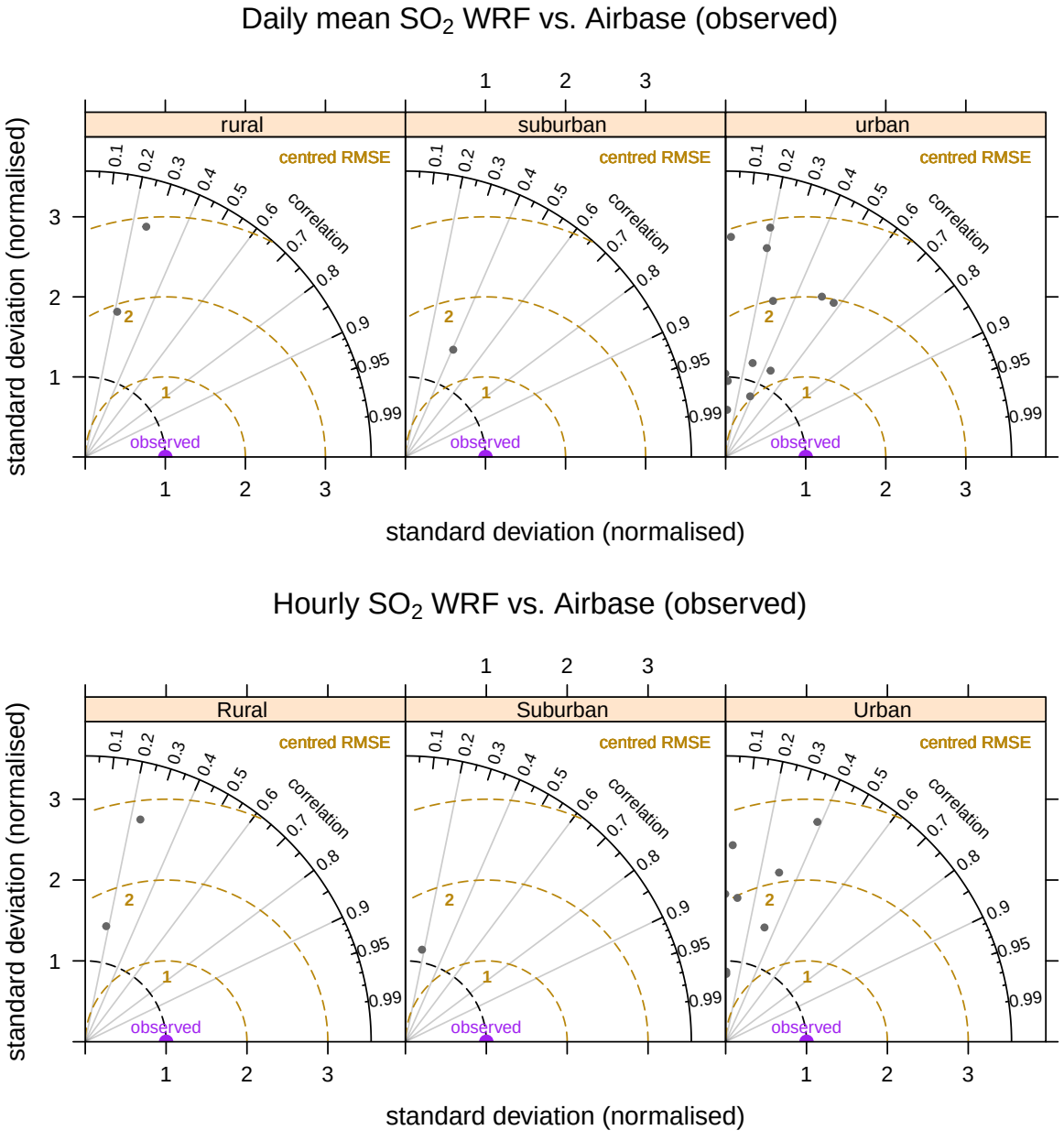


**Figure B4.** Evaluation of $SO_2$ concentration simulated by WRF-Chem using AirBase data. It remains a huge challenge to simulate the near-surface concentration $SO_2$. The model is prone to overestimate the $SO_2$ concentration, as the point source $SO_2$ emissions from inventories are assigned to the immediate surface. However, as $SO_2$ is not a major constituent in wildfire smokes, the resulting impacts on the conclusions of this study is considered minimal.

https://doi.org/10.5194/nhess-2023-111
Preprint. Discussion started: 18 July 2023


Natural Hazards and Earth System Sciences
Discussions

## Appendix C: Diurnal pattern of multi-month hourly mean concentration of air pollutants

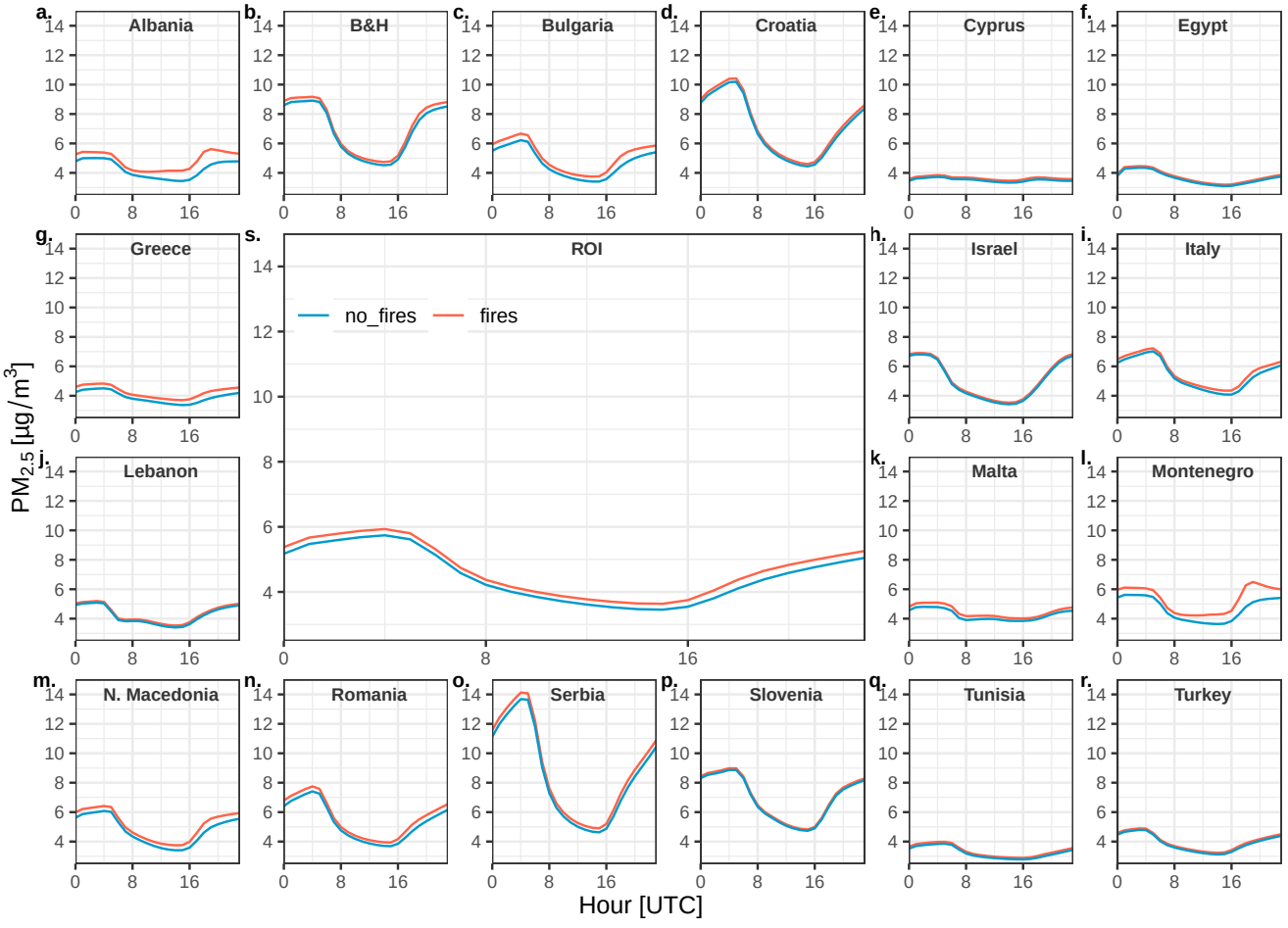


**Figure C1.** Diurnal pattern of multi-month hourly mean ambient $PM_{2.5}$ concentration for each country and the entire region of interest (ROI). In most countries, the $PM_{2.5}$ concentration follows a pattern subject to the mixing layer height. The daytime troughs reflect strong turbulent exchange and dilution within the mixed layer, whereas stable nighttime boundary layer enables $PM_{2.5}$ to accumulate Manning et al. (2018). The wildfire-caused elevation of $PM_{2.5}$ concentration in all countries can be ascribed to the emissions of gas-phase air pollutants such as $NO_x$, and VOCs from wildfires. These species are oxidized to form less volatile nitrates, and secondary organic aerosols (SOAs), respectively, and condense into the particle phase Kroll et al. (2020).

https://doi.org/10.5194/nhess-2023-111
Preprint. Discussion started: 18 July 2023


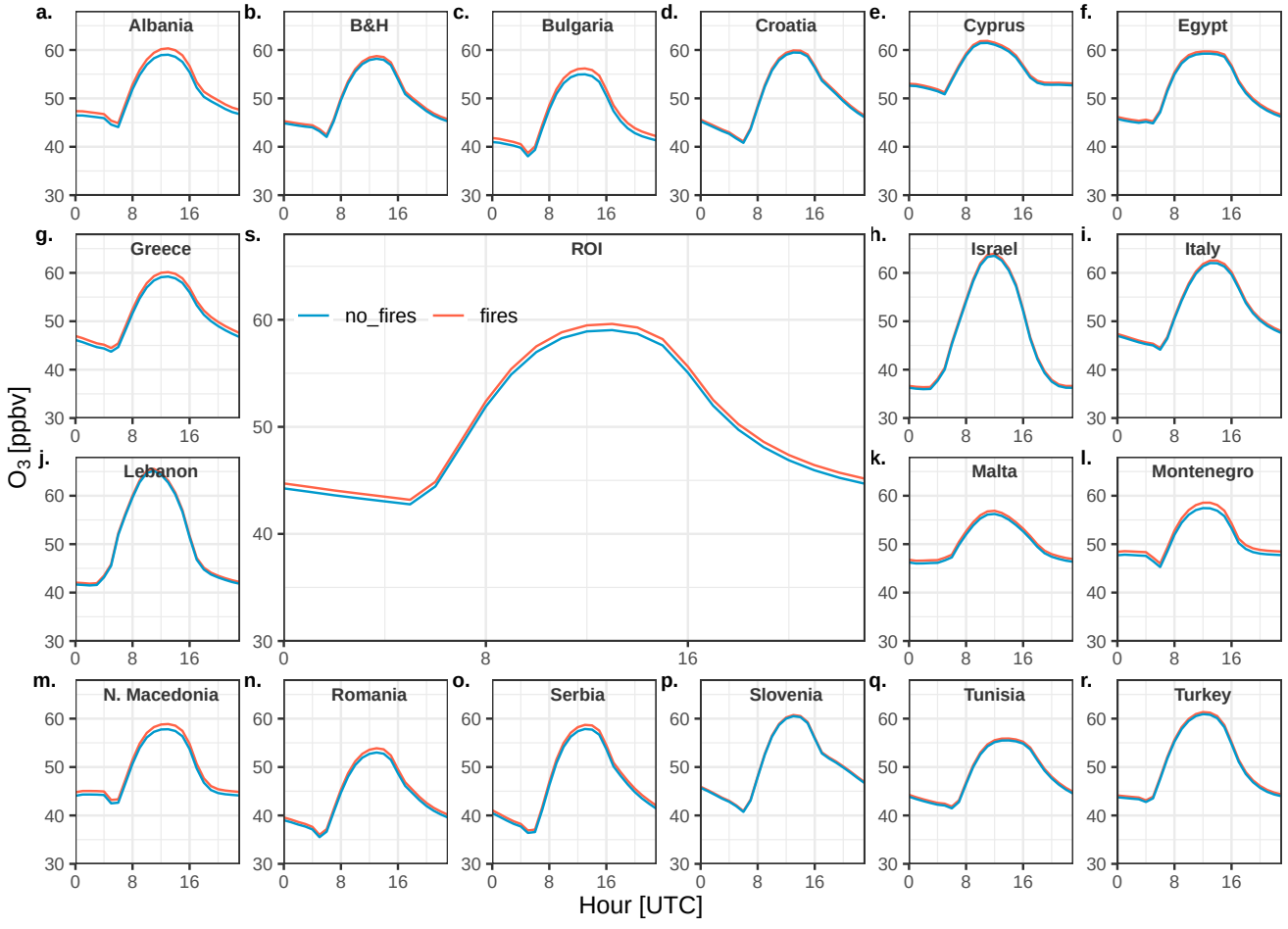


**Figure C2.** Diurnal pattern of multi-month hourly mean $O_3$ concentration for each country and the entire ROI. The biomass burning presents a significant source of $O_3$ precursors such as carbon monoxide (CO), volatile organic compounds (VOCs), and nitrogen oxide ($NO_x$), which form $O_3$ in the presence of solar radiation Holzinger et al. (1999). Therefore, the concentration of $O_3$ starts to increase after the sunrise and often reaches its maximum in the afternoon (between LT1200 and 1600). As the time of the day (horizontal axis) is in UTC, the local time (LT) of each country may be offset, subject to the time zone which the country is located in.

https://doi.org/10.5194/nhess-2023-111
Preprint. Discussion started: 18 July 2023


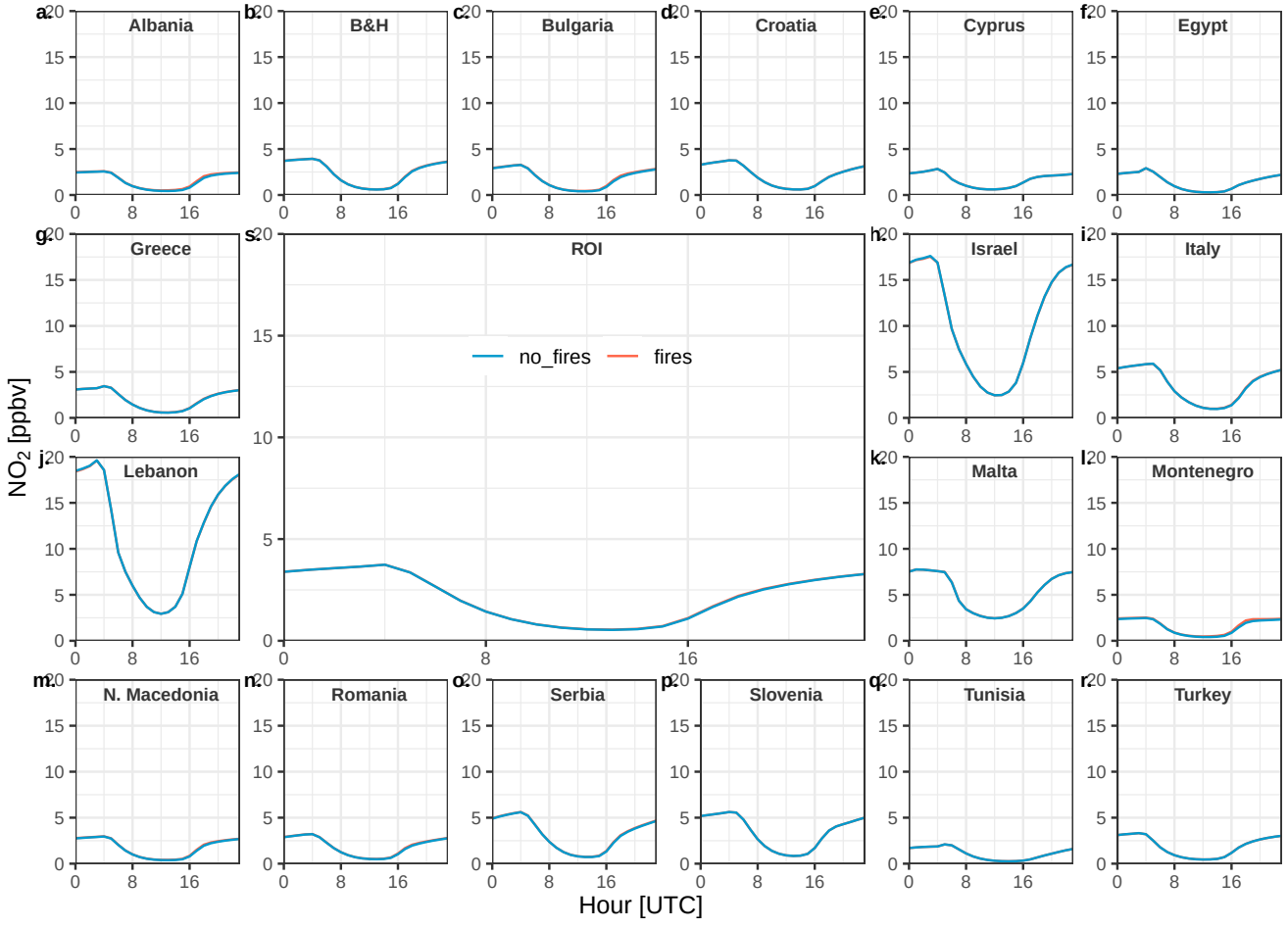


**Figure C3.** Diurnal pattern of multi-month hourly mean $NO_2$ concentration for each country and the entire region of interest.

https://doi.org/10.5194/nhess-2023-111
Preprint. Discussion started: 18 July 2023


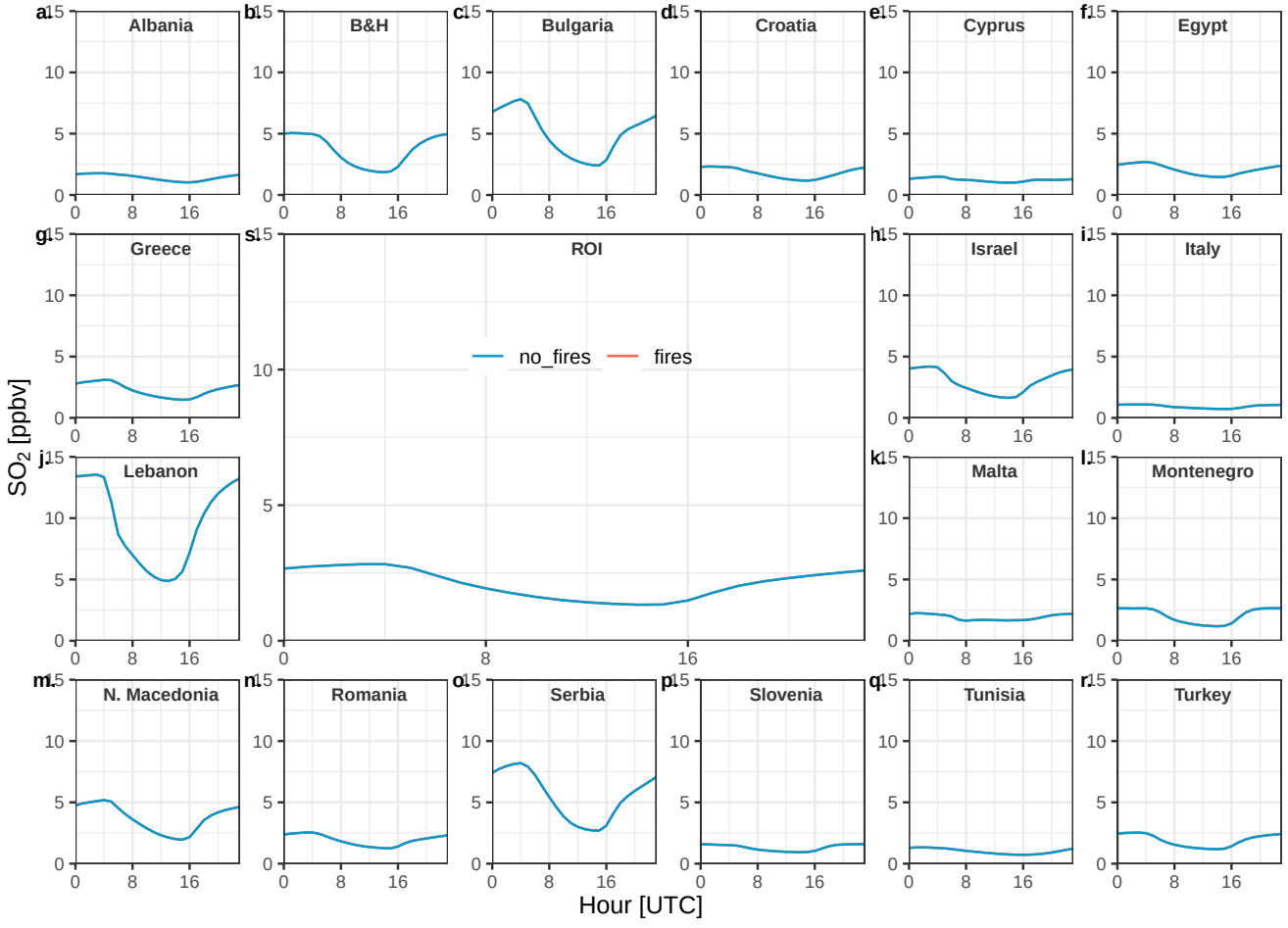


**Figure C4.** Diurnal pattern of multi-month hourly mean $SO_2$ concentration for each country and the entire region of interest.

https://doi.org/10.5194/nhess-2023-111
Preprint. Discussion started: 18 July 2023


Natural Hazards and Earth System Sciences
Discussions
Open Access
EGU

**Appendix D: Spatial pattern of WRF-simulated multi-month mean concentration of air pollutants**

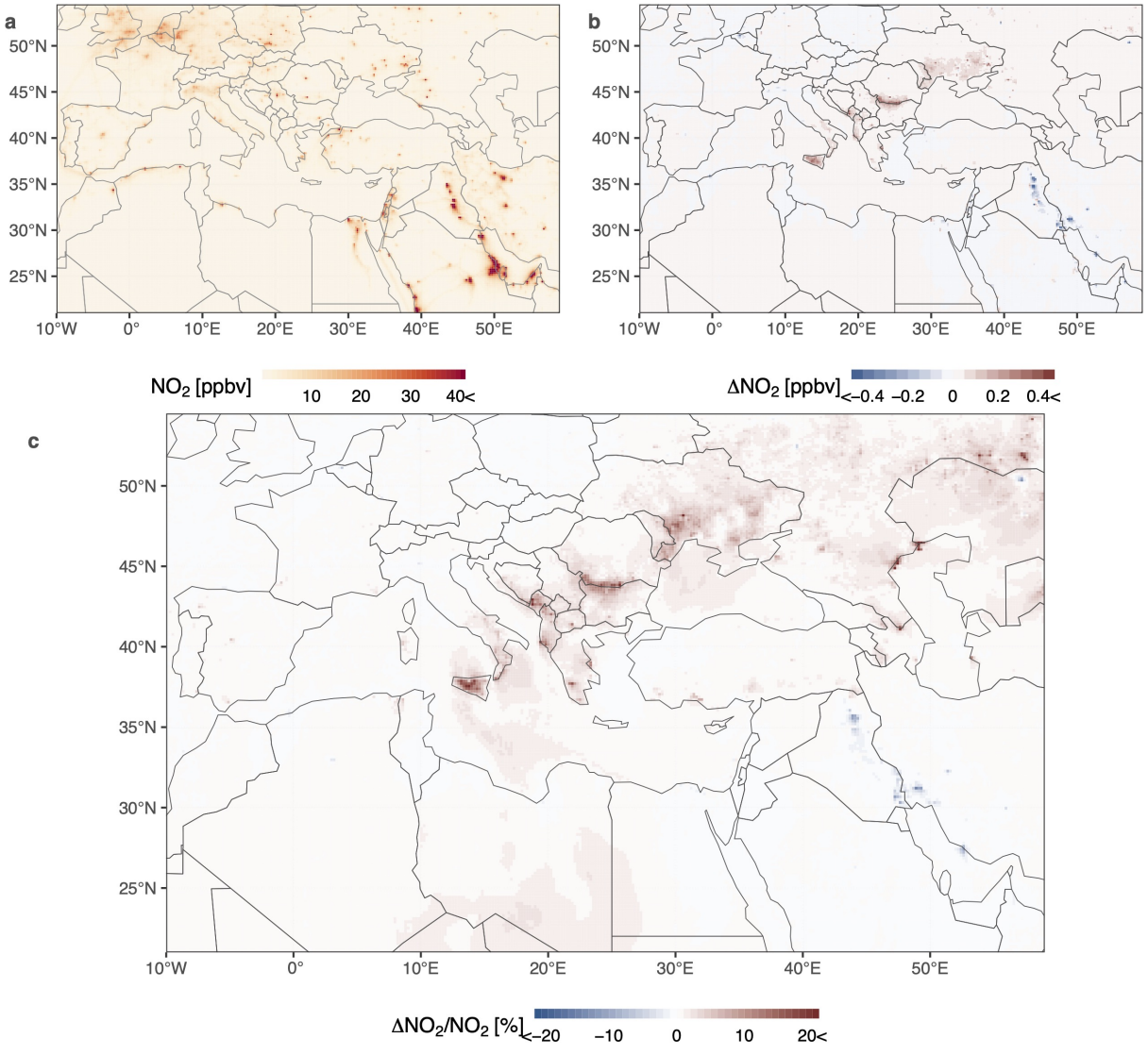


**Figure D1.** Spatial pattern of multi-month mean $NO_2$ concentration simulated by WRF-Chem under the fires scenario and the difference relative to the no-fires scenario. a) $NO_2$ concentration simulated with fires scenario, b) $NO_2$ concentration with fires scenario relative to no-fires ($\Delta NO_2 = NO_2^{fires} - NO_2^{no\text{-}fires}$), c) $NO_2$ concentration attributable to wildfires in percentages ($\Delta NO_2/NO_2^{fires}$).The elevation of wildfire-caused $NO_2$ is mainly observed in the Balkans, Greece, and South Italy.

https://doi.org/10.5194/nhess-2023-111
Preprint. Discussion started: 18 July 2023


Natural Hazards and Earth System Sciences
Discussions

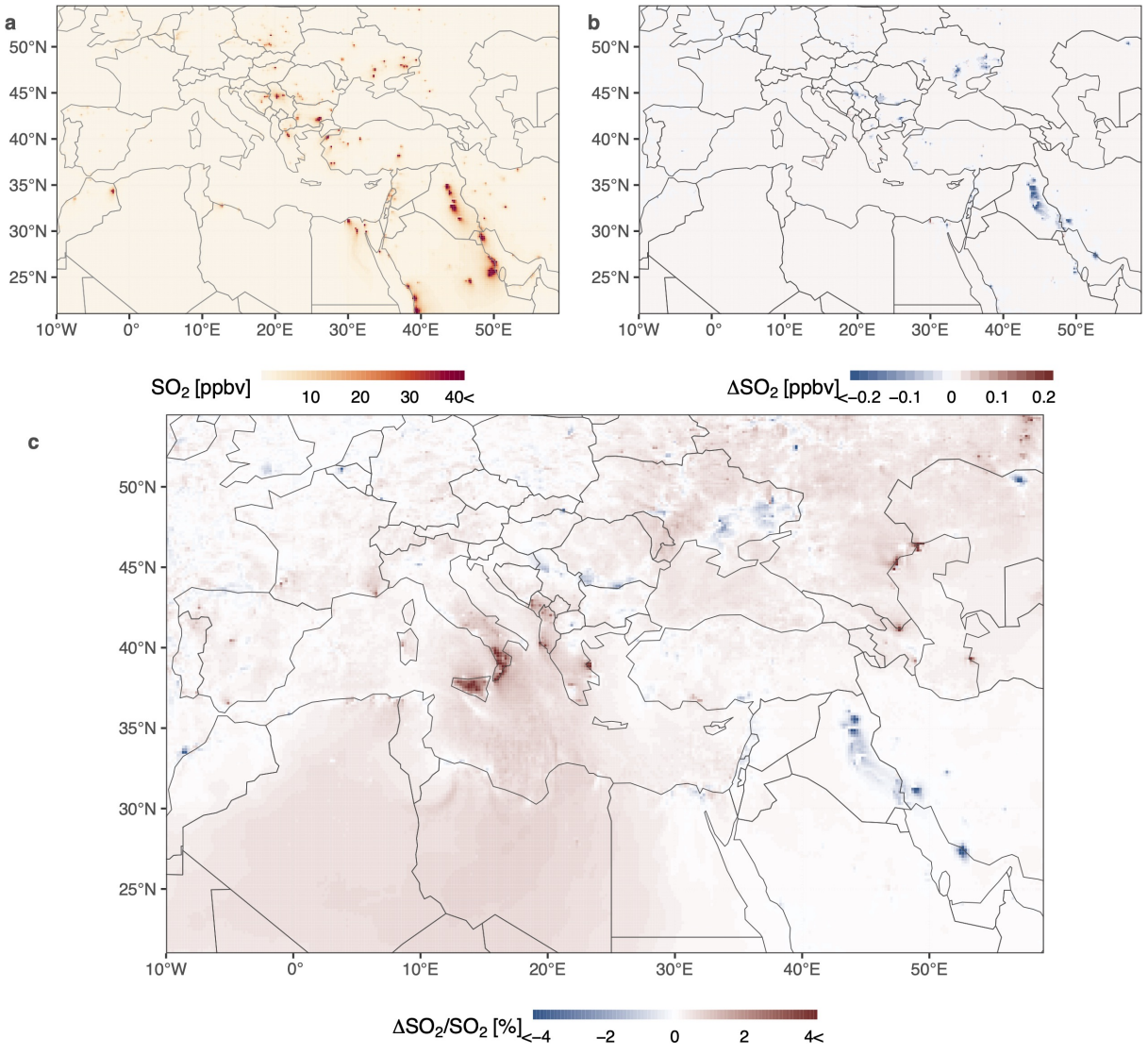


**Figure D2.** Spatial pattern of multi-month mean $SO_2$ concentration simulated by WRF-Chem under the fires scenario and the difference relative to the no-fires scenario. a) $SO_2$ concentration simulated with fires scenario, b) $SO_2$ concentration with fires scenario relative to no-fires ($\Delta SO_2 = SO_2^{fires} - SO_2^{no\text{-}fires}$), c) $SO_2$ concentration attributable to wildfires in percentages ($\Delta SO_2/SO_2^{fires}$). The elevation of wildfire-caused $SO_2$ is mainly observed in Albania, Greece and South Italy.

https://doi.org/10.5194/nhess-2023-111
Preprint. Discussion started: 18 July 2023




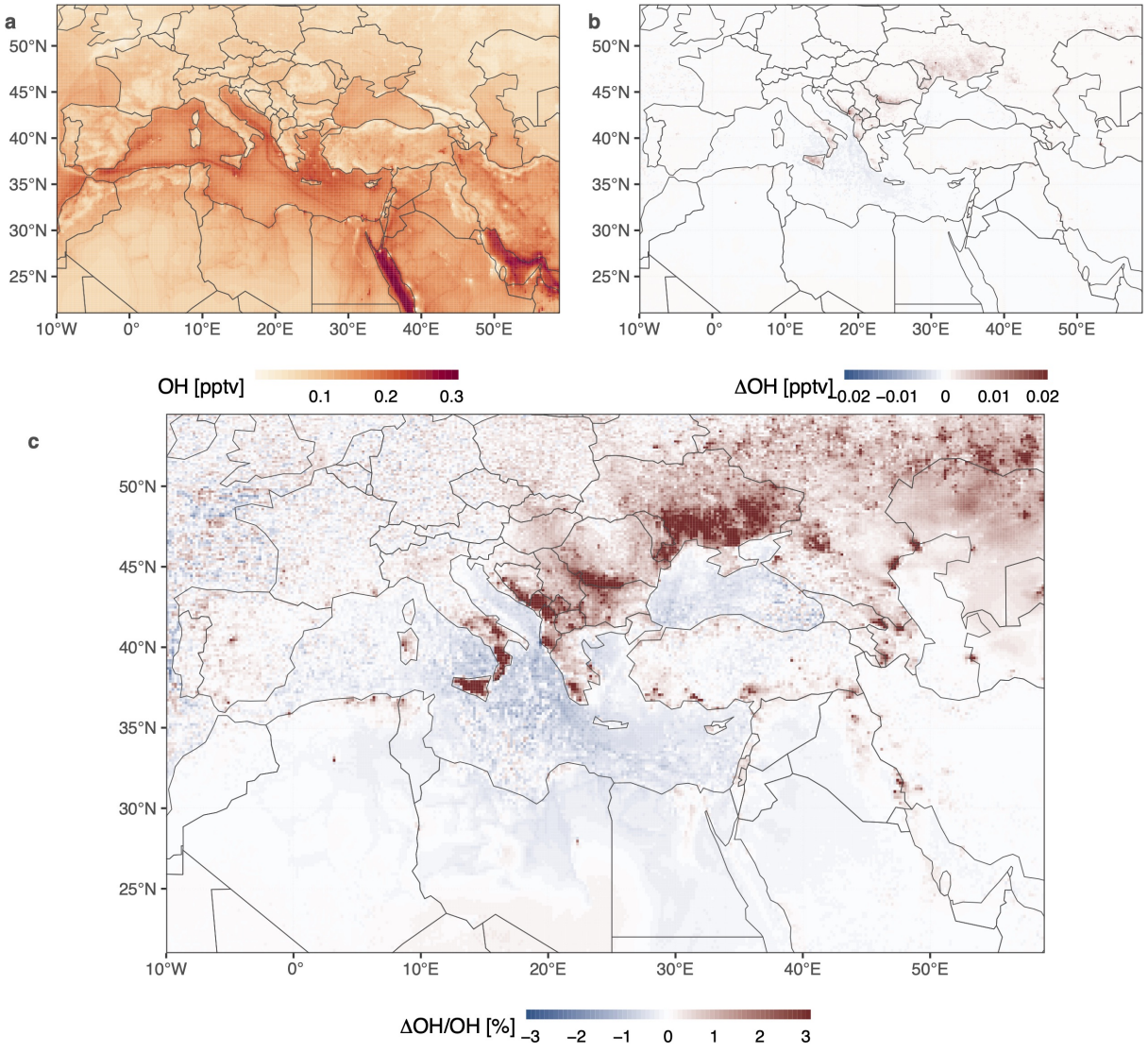


**Figure D3.** Spatial pattern of multi-month mean hydroxyl radical (OH) concentration simulated by WRF-Chem under the fires scenario and the difference relative to the no-fires scenario. a) OH concentration simulated with fires scenario, b) OH concentration with fires scenario relative to no-fires ($\Delta OH = OH^{fires} - OH^{no\text{-}fires}$), c) OH concentration attributable to wildfires in percentages ($\Delta OH/OH^{fires}$).

https://doi.org/10.5194/nhess-2023-111
Preprint. Discussion started: 18 July 2023


Natural Hazards and Earth System Sciences
Discussions

## Appendix E: Time series of population weighted concentration difference

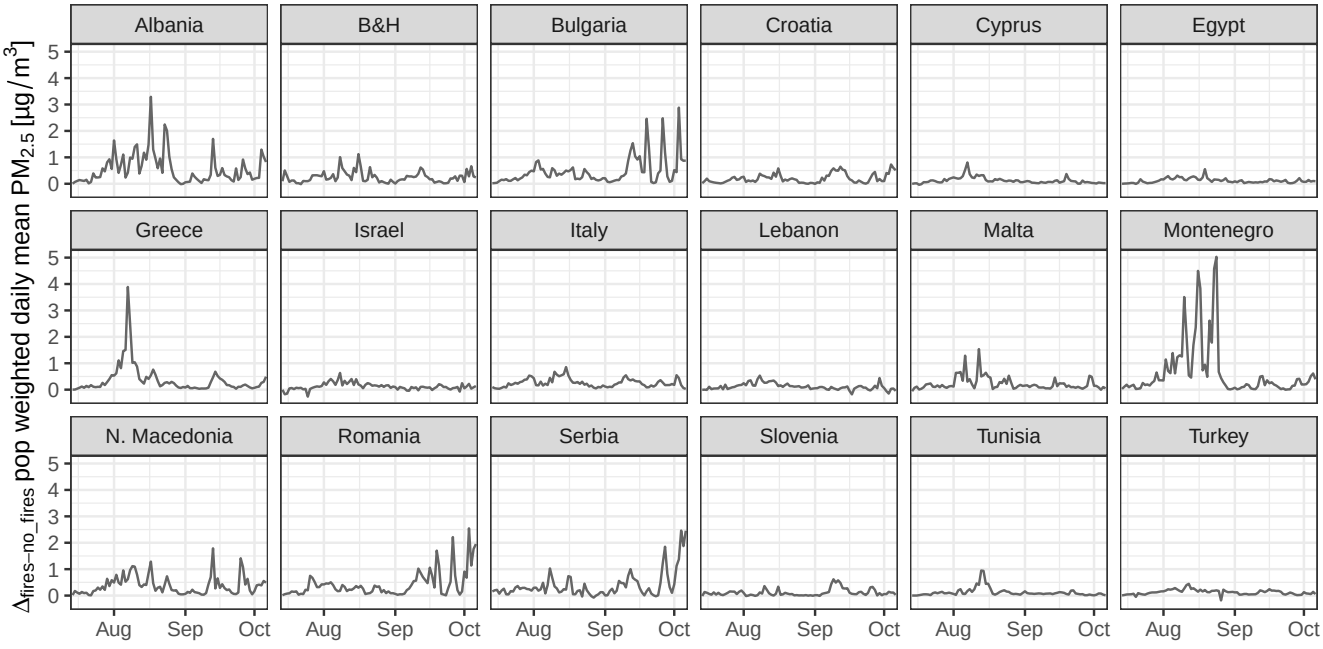


**Figure E1.** Time series of 24h-mean population weighted concentration difference of $PM_{2.5}$ (fires - no_fires) for each country.

https://doi.org/10.5194/nhess-2023-111
Preprint. Discussion started: 18 July 2023


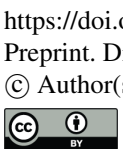

Natural Hazards and Earth System Sciences
Discussions

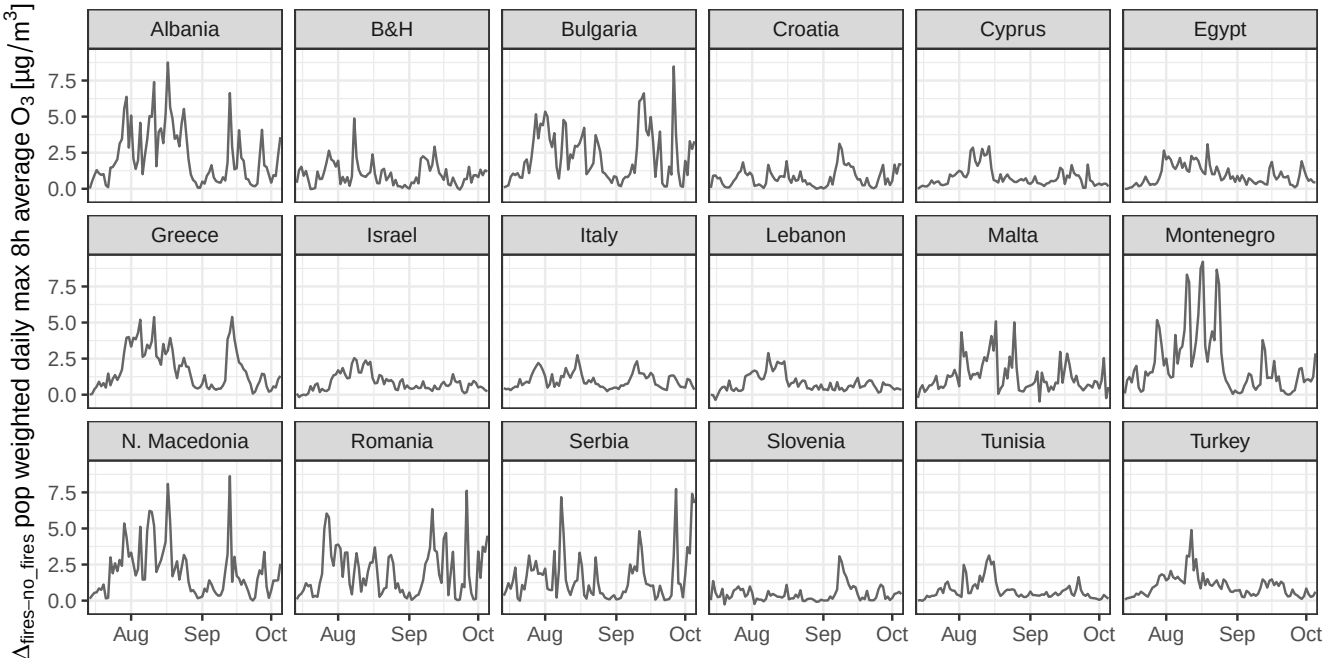


**Figure E2.** Time series of population weighted daily maximum 8-h average (DMA8) difference of $O_3$ (fires - no_fires) for each country.

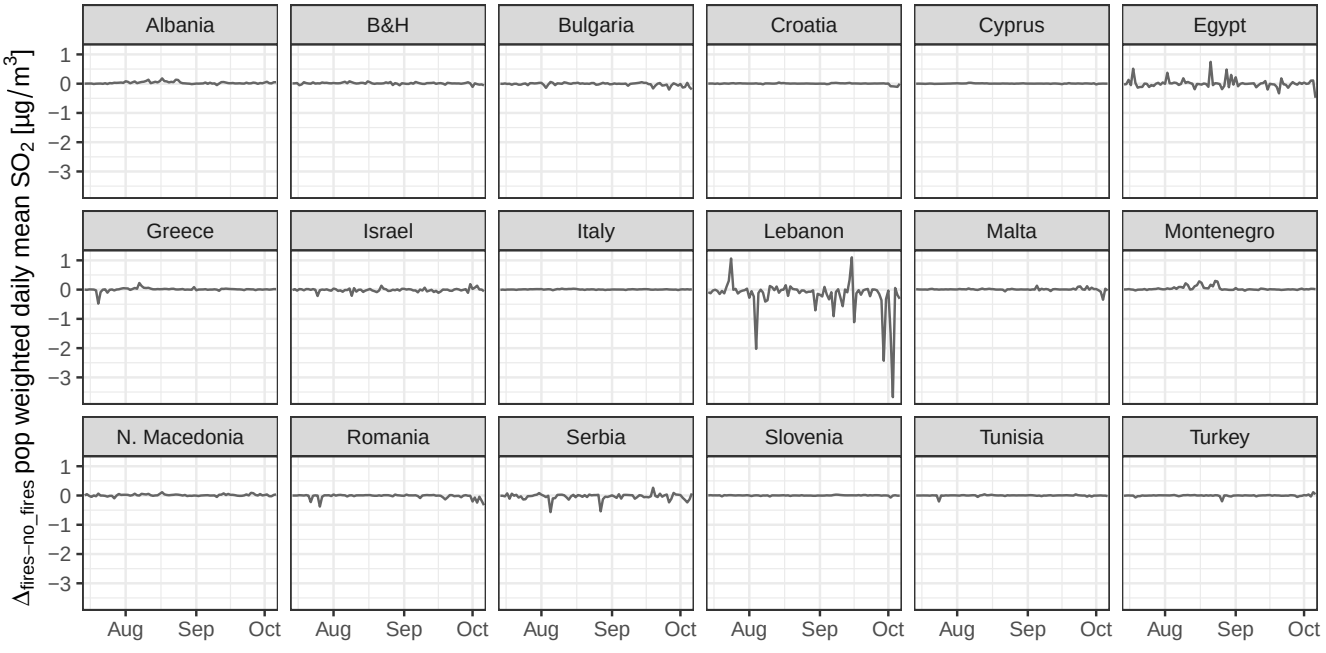


**Figure E3.** Time series of 24h-mean population weighted concentration difference of $SO_2$ (fires - no_fires) for each country.

https://doi.org/10.5194/nhess-2023-111
Preprint. Discussion started: 18 July 2023


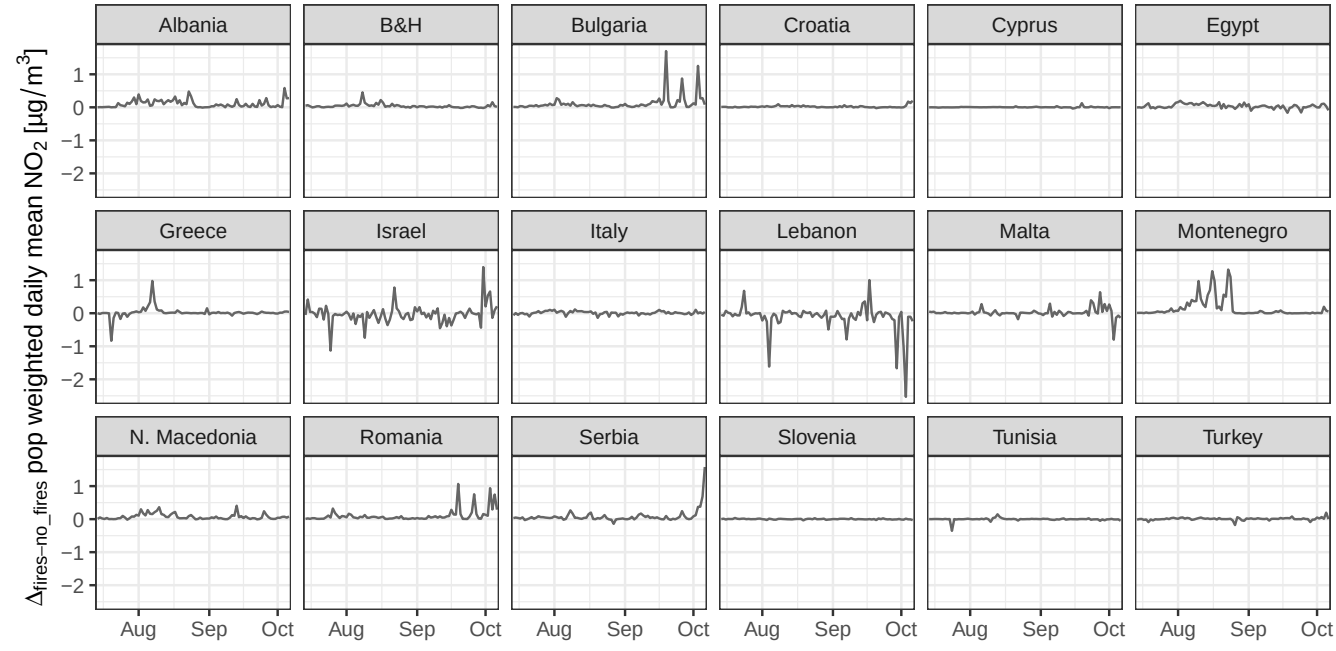


**Figure E4.** Time series of 24h-mean population weighted concentration difference of $NO_2$ (fires - no_fires) for each country.

https://doi.org/10.5194/nhess-2023-111
Preprint. Discussion started: 18 July 2023


Natural Hazards and Earth System Sciences
Discussions

*Data availability.* Original WRF-Chem simulation data are available upon request to the corresponding author.

*Code and data availability.* Data and code used for data analysis and visualization are available on Zenodo, https://doi.org/10.5281/zenodo.8120613

*Author contributions.* Both authors were involved in the study design and conceptualized the methodology. CK performed the WRF-Chem simulation. BZ curated, analysed and visualized the data. BZ wrote the original draft of the manuscript. CK reviewed and edited the manuscript. CK administrated the project and funding acquisition.

*Competing interests.* The authors declare no conflict of interest.

*Acknowledgements.* The authors acknowledge the European Forest Fire Information System of the European Commission for providing the data on total number of wildfires and total area of burnt areas. We acknowledge use of the WRF-Chem preprocessor tools mozbc, bio_emiss, fire_emiss and anthro_emiss provided by the Atmospheric Chemistry Observations and Modeling Lab (ACOM) of NCAR. The authors gratefully acknowledge computing time at the Augsburg Linux Compute Cluster (ALCC). Additional thanks go to Dr. David Jean du Preez for proofreading this paper.

https://doi.org/10.5194/nhess-2023-111
Preprint. Discussion started: 18 July 2023




## References

Akagi, S. K., Yokelson, R. J., Wiedinmyer, C., Alvarado, M. J., Reid, J. S., Karl, T., Crounse, J. D., and Wennberg, P. O.: Emission factors for open and domestic biomass burning for use in atmospheric models, Atmospheric Chemistry and Physics, 11, 4039–4072, https://doi.org/10.5194/acp-11-4039-2011, 2011.

Anderson, G. B., Krall, J. R., Peng, R. D., and Bell, M. L.: Is the relation between ozone and mortality confounded by chemical components of particulate matter? Analysis of 7 components in 57 US communities, American Journal of Epidemiology, 176, 726–732, https://doi.org/10.1093/aje/kws188, 2012.

Anenberg, S. C., Horowitz, L. W., Tong, D. Q., and West, J. J.: An estimate of the global burden of anthropogenic ozone and fine particulate matter on premature human mortality using atmospheric modeling, Environmental Health Perspectives, 118, 1189–1195, https://doi.org/10.1289/ehp.0901220, 2010.

Archer-Nicholls, S., Lowe, D., Darbyshire, E., Morgan, W. T., Bela, M. M., Pereira, G., Trembath, J., Kaiser, J. W., Longo, K. M., Freitas, S. R., Coe, H., and McFiggans, G.: Characterising Brazilian biomass burning emissions using WRF-Chem with MOSAIC sectional aerosol, Geoscientific Model Development, 8, 549–577, https://doi.org/10.5194/gmd-8-549-2015, 2015.

Bell, M. L., Kim, J. Y., and Dominici, F.: Potential confounding of particulate matter on the short-term association between ozone and mortality in multisite time-series studies, Environmental Health Perspectives, 115, 1591–1595, https://doi.org/10.1289/ehp.10108, 2007.

Bencherif, H., Bègue, N., Pinheiro, D. K., du Preez, D. J., Cadet, J. M., Lopes, F. J. d. S., Shikwambana, L., Landulfo, E., Vescovini, T., Labuschagne, C., Silva, J. J., Anabor, V., Coheur, P. F., Mbatha, N., Hadji-Lazaro, J., Sivakumar, V., and Clerbaux, C.: Investigating the long-range transport of aerosol plumes following the amazon fires (August 2019): A multi-instrumental approach from ground-based and satellite observations, Remote Sensing, 12, 1–18, https://doi.org/10.3390/rs12223846, 2020.

Bowman, D. M. J. S., Kolden, C. A., Abatzoglou, J. T., Johnston, F. H., van der Werf, G. R., and Flannigan, M.: Vegetation fires in the Anthropocene, Nature Reviews Earth & Environment, 1, 500–515, https://doi.org/10.1038/s43017-020-0085-3, 2020.

Brunekreef, B. and Holgate, S. T.: Air pollution and health, Lancet, 360, 1233–1242, https://doi.org/10.1016/S0140-6736(02)11274-8, 2002.

Burke, M., Driscoll, A., Heft-Neal, S., Xue, J., Burney, J., and Wara, M.: The changing risk and burden of wildfire in the United States, Proceedings of the National Academy of Sciences of the United States of America, 118, 1–6, https://doi.org/10.1073/PNAS.2011048118, 2021.

Burnett, R. T., Arden Pope, C., Ezzati, M., Olives, C., Lim, S. S., Mehta, S., Shin, H. H., Singh, G., Hubbell, B., Brauer, M., Ross Anderson, H., Smith, K. R., Balmes, J. R., Bruce, N. G., Kan, H., Laden, F., Prüss-Ustün, A., Turner, M. C., Gapstur, S. M., Diver, W. R., and Cohen, A.: An integrated risk function for estimating the global burden of disease attributable to ambient fine particulate matter exposure, Environmental Health Perspectives, 122, 397–403, https://doi.org/10.1289/ehp.1307049, 2014.

Butt, E. W., Conibear, L., Knote, C., and Spracklen, D. V.: Large Air Quality and Public Health Impacts due to Amazonian Deforestation Fires in 2019, GeoHealth, 5, 1–16, https://doi.org/10.1029/2021GH000429, 2021.

CAMS: Wildfires wreaked havoc in 2021, CAMS tracked their impact, https://atmosphere.copernicus.eu/wildfires-wreaked-havoc-2021-cams-tracked-their-impact(Accessed:2022-02-01), 2021.

Chen, G., Guo, Y., Yue, X., Tong, S., Gasparrini, A., Bell, M. L., Armstrong, B., Schwartz, J., Jaakkola, J. J. K., Zanobetti, A., Lavigne, E., Nascimento Saldiva, P. H., Kan, H., Royé, D., Milojevic, A., Overcenco, A., Urban, A., Schneider, A., Entezari, A., Vicedo-Cabrera, A. M., Zeka, A., Tobias, A., Nunes, B., Alahmad, B., Forsberg, B., Pan, S.-C., Íñiguez, C., Ameling, C., De la Cruz Valencia, C., Åström, C., Houthuijs, D., Van Dung, D., Samoli, E., Mayvaneh, F., Sera, F., Carrasco-Escobar, G., Lei, Y., Orru, H., Kim, H., Holobaca, I.-H.,

https://doi.org/10.5194/nhess-2023-111
Preprint. Discussion started: 18 July 2023




Kyselý, J., Teixeira, J. P., Madureira, J., Katsouyanni, K., Hurtado-Díaz, M., Maasikmets, M., Ragettli, M. S., Hashizume, M., Stafoggia, M., Pascal, M., Scortichini, M., de Sousa Zanotti Stagliorio Coêlho, M., Valdés Ortega, N., Ryti, N. R. I., Scovronick, N., Matus, P., Goodman, P., Garland, R. M., Abrutzky, R., Garcia, S. O., Rao, S., Fratianni, S., Dang, T. N., Colistro, V., Huber, V., Lee, W., Seposo, X., Honda, Y., Guo, Y. L., Ye, T., Yu, W., Abramson, M. J., Samet, J. M., and Li, S.: Mortality risk attributable to wildfire-related PM2·5 pollution: a global time series study in 749 locations, The Lancet Planetary Health, 5, e579–e587, https://doi.org/10.1016/S2542-5196(21)00200-X, 2021.

CIESIN: Gridded Population of the World, Version 4 (GPWv4): Population Count Adjusted to Match 2015 Revision of UN WPP Country Totals, Revision 11, https://doi.org/10.7927/H4PN93PB, 2018.

Cohen, A. J., Brauer, M., Burnett, R., Anderson, H. R., Frostad, J., Estep, K., Balakrishnan, K., Brunekreef, B., Dandona, L., Dandona, R., Feigin, V., Freedman, G., Hubbell, B., Jobling, A., Kan, H., Knibbs, L., Liu, Y., Martin, R., Morawska, L., Pope, C. A., Shin, H., Straif, K., Shaddick, G., Thomas, M., van Dingenen, R., van Donkelaar, A., Vos, T., Murray, C. J., and Forouzanfar, M. H.: Estimates and 25-year trends of the global burden of disease attributable to ambient air pollution: an analysis of data from the Global Burden of Diseases Study 2015, The Lancet, 389, 1907–1918, https://doi.org/10.1016/S0140-6736(17)30505-6, 2017.

Conibear, L., Reddington, C. L., Silver, B. J., Chen, Y., Knote, C., Arnold, S. R., and Spracklen, D. V.: Statistical Emulation of Winter Ambient Fine Particulate Matter Concentrations From Emission Changes in China, GeoHealth, 5, 1–13, https://doi.org/10.1029/2021GH000391, 2021.

Cos, J., Doblas-Reyes, F., Jury, M., Marcos, R., Bretonnière, P.-A., and Samsó, M.: The Mediterranean climate change hotspot in the CMIP5 and CMIP6 projections, Earth System Dynamics Discussions, pp. 1–26, https://doi.org/10.5194/esd-2021-65, 2021.

Crippa, M., Guizzardi, D., Muntean, M., and Schaaf, E.: EDGAR v5.0 Global Air Pollutant Emissions, http://data.europa.eu/89h/377801af-b094-4943-8fdc-f79a7c0c2d19, 2021.

Di, Q., Amini, H., Shi, L., Kloog, I., Silvern, R., Kelly, J., Sabath, M. B., Choirat, C., Koutrakis, P., Lyapustin, A., Wang, Y., Mickley, L. J., and Schwartz, J.: An ensemble-based model of PM2.5 concentration across the contiguous United States with high spatiotemporal resolution, Environment International, 130, 104 909, https://doi.org/10.1016/j.envint.2019.104909, 2019.

Dong, T. T., Hinwood, A. L., Callan, A. C., Zosky, G., and Stock, W. D.: In vitro assessment of the toxicity of bushfire emissions: A review, Science of the Total Environment, 603-604, 268–278, https://doi.org/10.1016/j.scitotenv.2017.06.062, 2017.

EFFIS: Total burnt areas and total number of fires in 2021., https://effis.jrc.ec.europa.eu/applications/data-and-services(accessed: 2021-12-01), 2021.

Emmons, L. K., Walters, S., Hess, P. G., Lamarque, J.-F., Pfister, G. G., Fillmore, D., Granier, C., Guenther, A., Kinnison, D., Laepple, T., Orlando, J., Tie, X., Tyndall, G., Wiedinmyer, C., Baughcum, S. L., and Kloster, S.: Description and evaluation of the Model for Ozone and Related chemical Tracers, version 4 (MOZART-4), Geoscientific Model Development, 3, 43–67, https://doi.org/10.5194/gmd-3-43-2010, 2010.

European Environment Agency: AirBase air quality data (E1a & E2a), https://discomap.eea.europa.eu/map/fme/AirQualityExport.htm, 2021.

Eurostat: Deaths (total) by month, 2010-2019, 2021.

Evangelopoulos, D., Katsouyanni, K., Keogh, R. H., Samoli, E., Schwartz, J., Barratt, B., Zhang, H., and Walton, H.: PM2.5 and NO2 exposure errors using proxy measures, including derived personal exposure from outdoor sources: A systematic review and meta-analysis, Environment International, 137, 105 500, https://doi.org/10.1016/j.envint.2020.105500, 2020.

Fann, N., Alman, B., Broome, R. A., Morgan, G. G., Johnston, F. H., Pouliot, G., and Rappold, A. G.: The health impacts and economic value of wildland fire episodes in the US: 2008–2012, Science of the total environment, 610, 802–809, 2018.

https://doi.org/10.5194/nhess-2023-111
Preprint. Discussion started: 18 July 2023




Freitas, S. R., Longo, K. M., Chatfield, R., Latham, D., Silva Dias, M. A. F., Andreae, M. O., Prins, E., Santos, J. C., Gielow, R., and Carvalho Jr., J. A.: Including the sub-grid scale plume rise of vegetation fires in low resolution atmospheric transport models, Atmospheric Chemistry and Physics, 7, 3385–3398, https://doi.org/10.5194/acp-7-3385-2007, 2007.

Global Burden of Disease Collaborative Network: Global Burden of Disease Study 2019 (GBD 2019) Results., http://ghdx.healthdata.org/gbd-results-tool?params=gbd-api-2019-permalink/4e1860d6fad20ccf64c5e6f7e1f7a24b, 2020.

Gong, S.: A parameterization of sea-salt aerosol source function for sub-and super-micron particles, Global biogeochemical cycles, 17, 2003.

Graham, A. M., Pringle, K. J., Pope, R. J., Arnold, S. R., Conibear, L. A., Burns, H., Rigby, R., Borchers-Arriagada, N., Butt, E. W., Kiely, L., Reddington, C., Spracklen, D. V., Woodhouse, M. T., Knote, C., and McQuaid, J. B.: Impact of the 2019/2020 Australian Megafires on Air Quality and Health, GeoHealth, 5, 1–17, https://doi.org/10.1029/2021GH000454, 2021.

Grell, G. A., Peckham, S. E., Schmitz, R., McKeen, S. A., Frost, G., Skamarock, W. C., and Eder, B.: Fully coupled "online" chemistry within the WRF model, Atmospheric Environment, 39, 6957–6975, 2005.

Guenther, A., Karl, T., Harley, P., Wiedinmyer, C., Palmer, P. I., and Geron, C.: Estimates of global terrestrial isoprene emissions using MEGAN (Model of Emissions of Gases and Aerosols from Nature), Atmospheric Chemistry and Physics, 6, 3181–3210, 2006.

Haikerwal, A., Akram, M., Monaco, A. D., Smith, K., Sim, M. R., Meyer, M., Tonkin, A. M., Abramson, M. J., and Dennekamp, M.: Impact of fine particulate matter (PM2.5) exposure during wildfires on cardiovascular health outcomes, Journal of the American Heart Association, 4, 1–10, https://doi.org/10.1161/JAHA.114.001653, 2015.

Hobbs, P. V., Sinha, P., Yokelson, R. J., Christian, T. J., Blake, D. R., Gao, S., Kirchstetter, T. W., Novakov, T., and Pilewskie, P.: Evolution of gases and particles from a savanna fire in South Africa, Journal of Geophysical Research: Atmospheres, 108, https://doi.org/10.1029/2002jd002352, 2003.

Hodzic, A. and Jimenez, J. L.: Modeling anthropogenically controlled secondary organic aerosols in a megacity: a simplified framework for global and climate models, Geoscientific Model Development, 4, 901–917, https://doi.org/10.5194/gmd-4-901-2011, 2011.

Holzinger, R., Wameke, C., Hansel, A., Jordan, A., Lindinger, W., Scharffe, D. H., Schade, G., and Crutzen, P. J.: Biomass burning as a source of formaldehyde, acetaldehyde, methanol, acetone, acetonitrile, and hydrogen cyanide, Geophysical Research Letters, 26, 1161–1164, https://doi.org/10.1029/1999GL900156, 1999.

Hough, I., Sarafian, R., Shtein, A., Zhou, B., Lepeule, J., and Kloog, I.: Gaussian Markov random fields improve ensemble predictions of daily 1 km PM2.5 and PM10 across France, Atmospheric Environment, 264, 118 693, https://doi.org/10.1016/j.atmosenv.2021.118693, 2021.

Im, U., Bianconi, R., Solazzo, E., Kioutsioukis, I., Badia, A., Balzarini, A., Baró, R., Bellasio, R., Brunner, D., Chemel, C., Curci, G., Denier van der Gon, H., Flemming, J., Forkel, R., Giordano, L., Jiménez-Guerrero, P., Hirtl, M., Hodzic, A., Honzak, L., Jorba, O., Knote, C., Makar, P. A., Manders-Groot, A., Neal, L., Pérez, J. L., Pirovano, G., Pouliot, G., San Jose, R., Savage, N., Schroder, W., Sokhi, R. S., Syrakov, D., Torian, A., Tuccella, P., Wang, K., Werhahn, J., Wolke, R., Zabkar, R., Zhang, Y., Zhang, J., Hogrefe, C., and Galmarini, S.: Evaluation of operational online-coupled regional air quality models over Europe and North America in the context of AQMEII phase 2. Part II: Particulate matter, Atmospheric Environment, 115, 421–441, https://doi.org/10.1016/j.atmosenv.2014.08.072, 2015a.

Im, U., Bianconi, R., Solazzo, E., Kioutsioukis, I., Badia, A., Balzarini, A., Baró, R., Bellasio, R., Brunner, D., Chemel, C., Curci, G., Flemming, J., Forkel, R., Giordano, L., Jiménez-Guerrero, P., Hirtl, M., Hodzic, A., Honzak, L., Jorba, O., Knote, C., Kuenen, J. J., Makar, P. A., Manders-Groot, A., Neal, L., Pérez, J. L., Pirovano, G., Pouliot, G., San Jose, R., Savage, N., Schroder, W., Sokhi, R. S., Syrakov, D., Torian, A., Tuccella, P., Werhahn, J., Wolke, R., Yahya, K., Zabkar, R., Zhang, Y., Zhang, J., Hogrefe, C., and Galmarini, S.:

https://doi.org/10.5194/nhess-2023-111
Preprint. Discussion started: 18 July 2023




Evaluation of operational on-line-coupled regional air quality models over Europe and North America in the context of AQMEII phase 2. Part I: Ozone, Atmospheric Environment, 115, 404–420, https://doi.org/10.1016/j.atmosenv.2014.09.042, 2015b.

Im, U., Brandt, J., Geels, C., Hansen, K. M., Christensen, J. H., Andersen, M. S., Solazzo, E., Kioutsioukis, I., Alyuz, U., Balzarini, A., Baro, R., Bellasio, R., Bianconi, R., Bieser, J., Colette, A., Curci, G., Farrow, A., Flemming, J., Fraser, A., Jimenez-Guerrero, P., Kitwiroon, N., Liang, C.-K., Nopmongcol, U., Pirovano, G., Pozzoli, L., Prank, M., Rose, R., Sokhi, R., Tuccella, P., Unal, A., Vivanco, M. G., West, J., Yarwood, G., Hogrefe, C., and Galmarini, S.: Assessment and economic valuation of air pollution impacts on human health over Europe and the United States as calculated by a multi-model ensemble in the framework of AQMEII3, Atmospheric Chemistry and Physics, 18, 5967–5989, https://doi.org/10.5194/acp-18-5967-2018, 2018.

Jaffe, D. A. and Wigder, N. L.: Ozone production from wildfires: A critical review, Atmospheric Environment, 51, 1–10, https://doi.org/10.1016/j.atmosenv.2011.11.063, 2012.

Johnston, F. H., Henderson, S. B., Chen, Y., Randerson, J. T., Marlier, M., DeFries, R. S., Kinney, P., Bowman, D. M., and Brauer, M.: Estimated Global Mortality Attributable to Smoke from Landscape Fires, Environmental Health Perspectives, 120, 695–701, https://doi.org/10.1289/ehp.1104422, 2012.

Jolly, W. M., Cochrane, M. A., Freeborn, P. H., Holden, Z. A., Brown, T. J., Williamson, G. J., and Bowman, D. M.: Climate-induced variations in global wildfire danger from 1979 to 2013, Nature Communications, 6, 1–11, https://doi.org/10.1038/ncomms8537, 2015.

Knote, C., Hodzic, A., Jimenez, J. L., Volkamer, R., Orlando, J. J., Baidar, S., Brioude, J., Fast, J., Gentner, D. R., Goldstein, A. H., Hayes, P. L., Knighton, W. B., Oetjen, H., Setyan, A., Stark, H., Thalman, R., Tyndall, G., Washenfelder, R., Waxman, E., and Zhang, Q.: Simulation of semi-explicit mechanisms of SOA formation from glyoxal in aerosol in a 3-D model, Atmospheric Chemistry and Physics, 14, 6213–6239, https://doi.org/10.5194/acp-14-6213-2014, 2014.

Knote, C., Hodzic, A., and Jimenez, J. L.: The effect of dry and wet deposition of condensable vapors on secondary organic aerosols concentrations over the continental US, Atmospheric Chemistry and Physics, 15, 1–18, https://doi.org/10.5194/acp-15-1-2015, 2015.

Kramer, H. A., Mockrin, M. H., Alexandre, P. M., and Radeloff, V. C.: High wildfire damage in interface communities in California, International Journal of Wildland Fire, 28, 641–650, https://doi.org/10.1071/WF18108, 2019.

Kroll, J. H., Heald, C. L., Cappa, C. D., Farmer, D. K., Fry, J. L., Murphy, J. G., and Steiner, A. L.: The complex chemical effects of COVID-19 shutdowns on air quality, Nature Chemistry, 12, 777–779, https://doi.org/10.1038/s41557-020-0535-z, 2020.

LeGrand, S. L., Polashenski, C., Letcher, T. W., Creighton, G. A., Peckham, S. E., and Cetola, J. D.: The AFWA dust emission scheme for the GOCART aerosol model in WRF-Chem v3. 8.1, Geoscientific Model Development, 12, 131–166, 2019.

Lelieveld, J., Pozzer, A., Pöschl, U., Fnais, M., Haines, A., and Münzel, T.: Loss of life expectancy from air pollution compared to other risk factors: A worldwide perspective, Cardiovascular Research, 116, 1910–1917, https://doi.org/10.1093/cvr/cvaa025, 2020.

Liang, C. K., West, J. J., Silva, R. A., Bian, H., Chin, M., Davila, Y., Dentener, F. J., Emmons, L., Flemming, J., Folberth, G., Henze, D., Im, U., Jonson, J. E., Keating, T. J., Kucsera, T., Lenzen, A., Lin, M., Tronstad Lund, M., Pan, X., Park, R. J., Pierce, R. B., Sekiya, T., Sudo, K., and Takemura, T.: HTAP2 multi-model estimates of premature human mortality due to intercontinental transport of air pollution and emission sectors, Atmospheric Chemistry and Physics, 18, 10 497–10 520, https://doi.org/10.5194/acp-18-10497-2018, 2018.

Linares, C., Díaz, J., Negev, M., Martínez, G. S., Debono, R., and Paz, S.: Impacts of climate change on the public health of the Mediterranean Basin population - Current situation, projections, preparedness and adaptation, Environmental Research, 182, 109 107, https://doi.org/10.1016/j.envres.2019.109107, 2020.

Liu, C., Chen, R., Sera, F., Vicedo-Cabrera, A. M., Guo, Y. Y.-L., Tong, S., Coelho, M. S., Saldiva, P. H., Lavigne, E., Matus, P., Valdes Ortega, N., Osorio Garcia, S., Pascal, M., Stafoggia, M., Scortichini, M., Hashizume, M., Honda, Y., Hurtado-Díaz, M., Cruz, J., Nunes,

https://doi.org/10.5194/nhess-2023-111
Preprint. Discussion started: 18 July 2023




B., Teixeira, J. P., Kim, H., Tobias, A., Íñiguez, C., Forsberg, B., Åström, C., Ragettli, M. S., Guo, Y. Y.-L., Chen, B.-Y., Bell, M. L., Wright, C. Y., Scovronick, N., Garland, R. M., Milojevic, A., Kyselý, J., Urban, A., Orru, H., Indermitte, E., Jaakkola, J. J., Ryti, N. R., Katsouyanni, K., Analitis, A., Zanobetti, A., Schwartz, J., Chen, J., Wu, T., Cohen, A., Gasparrini, A., and Kan, H.: Ambient Particulate Air Pollution and Daily Mortality in 652 Cities, New England Journal of Medicine, 381, 705–715, https://doi.org/10.1056/nejmoa1817364, 2019.

Lu, F., Xu, D., Cheng, Y., Dong, S., Guo, C., Jiang, X., and Zheng, X.: Systematic review and meta-analysis of the adverse health effects of ambient PM2.5 and PM10 pollution in the Chinese population, Environmental Research, 136, 196–204, https://doi.org/10.1016/j.envres.2014.06.029, 2015.

Macintyre, H. L., Heaviside, C., Neal, L. S., Agnew, P., Thornes, J., and Vardoulakis, S.: Mortality and emergency hospitalizations associated with atmospheric particulate matter episodes across the UK in spring 2014, Environment International, 97, 108–116, https://doi.org/10.1016/j.envint.2016.07.018, 2016.

Manning, M. I., Martin, R. V., Hasenkopf, C., Flasher, J., and Li, C.: Diurnal Patterns in Global Fine Particulate Matter Concentration, Environmental Science and Technology Letters, 5, 687–691, https://doi.org/10.1021/acs.estlett.8b00573, 2018.

Mansournia, M. A. and Altman, D. G.: Population attributable fraction, BMJ (Online), 360, 2–3, https://doi.org/10.1136/bmj.k757, 2018.

Naeher, L. P., Brauer, M., Lipsett, M., Zelikoff, J. T., Simpson, C. D., Koenig, J. Q., and Smith, K. R.: Woodsmoke health effects: A review, Inhalation Toxicology, 19, 67–106, https://doi.org/10.1080/08958370600985875, 2007.

Orellano, P., Reynoso, J., Quaranta, N., Bardach, A., and Ciapponi, A.: Short-term exposure to particulate matter (PM10 and PM2.5), nitrogen dioxide (NO2), and ozone (O3) and all-cause and cause-specific mortality: Systematic review and meta-analysis, Environment International, 142, 105 876, https://doi.org/10.1016/j.envint.2020.105876, 2020.

Page, M. J., Sterne, J. A. C., Higgins, J. P. T., and Egger, M.: Investigating and dealing with publication bias and other reporting biases in meta-analyses of health research: A review, Research Synthesis Methods, 12, 248–259, https://doi.org/10.1002/jrsm.1468, 2021.

Pebesma, E.: Simple Features for R: Standardized Support for Spatial Vector Data, The R Journal, 10, 439–446, https://doi.org/10.32614/RJ-2018-009, 2018.

R Core Team: R: A Language and Environment for Statistical Computing, R Foundation for Statistical Computing, Vienna, Austria, https://www.R-project.org/, 2021.

Ruffault, J., Curt, T., Moron, V., Trigo, R. M., Mouillot, F., Koutsias, N., Pimont, F., Martin-StPaul, N., Barbero, R., Dupuy, J. L., Russo, A., and Belhadj-Khedher, C.: Increased likelihood of heat-induced large wildfires in the Mediterranean Basin, Scientific Reports, 10, 1–9, https://doi.org/10.1038/s41598-020-70069-z, 2020.

Rutledge, G. K., Alpert, J., and Ebisuzaki, W.: NOMADS: A climate and weather model archive at the National Oceanic and Atmospheric Administration, Bulletin of the American Meteorological Society, 87, 327–341, https://doi.org/10.1175/BAMS-87-3-327, 2006.

San-Miguel-Ayanz, J., Durrant, T., Boca, R., Maianti, P., Liberta', P., Artes Vivancos, T., Jacome Felix Oom, D. P., Branco, A., De Rigo, D., Ferrari, D., Pfeiffer, H., Grecchi, R., Nuijten, D., Onida, M., and Loffler, P.: Advance Report on Forest Fires in Europe, Middle East and North Africa 2021, Tech. rep., https://doi.org/10.2760/039729, 2022.

Schneider, S. R. and Abbatt, J. P.: Wildfire atmospheric chemistry: climate and air quality impacts, Trends in Chemistry, 4, 255–257, https://doi.org/https://doi.org/10.1016/j.trechm.2021.12.004, special Issue: Third Anniversary, 2022.

Schwarz, L., Dimitrova, A., Aguilera, R., Basu, R., Gershunov, A., and Benmarhnia, T.: Smoke and COVID-19 case fatality ratios during California wildfires, Environmental Research Letters, 17, 014 054, https://doi.org/10.1088/1748-9326/ac4538, 2022.

https://doi.org/10.5194/nhess-2023-111
Preprint. Discussion started: 18 July 2023




Shtein, A., Kloog, I., Schwartz, J., Silibello, C., Michelozzi, P., Gariazzo, C., Viegi, G., Forastiere, F., Karnieli, A., Just, A. C., and Stafoggia, M.: Estimating daily PM2.5 and PM10 over Italy using an ensemble model, Environmental Science and Technology, 54, acs.est.9b04 279, https://doi.org/10.1021/acs.est.9b04279, 2019.

Sillman, S.: The relation between ozone, NOx and hydrocarbons in urban and polluted rural environments, Atmospheric Environment, 33, 1821–1845, https://doi.org/10.1016/S1352-2310(98)00345-8, 1999.

Stafoggia, M., Breitner, S., Hampel, R., and Basagaña, X.: Statistical Approaches to Address Multi-Pollutant Mixtures and Multiple Exposures: the State of the Science, Current environmental health reports, 4, 481–490, https://doi.org/10.1007/s40572-017-0162-z, 2017.

Task Force on Hemispheric Transport of Air Pollution (TF HTAP): Hemispheric Transport of Air Pollution 2010. Part A: Ozone and Particulate Matter. Air Pollution Studies No. 17, 17, 2010.

Taylor, K. E.: Summarizing multiple aspects of model performance in a single diagram, Journal of Geophysical Research: Atmospheres, 106, 7183–7192, https://doi.org/10.1029/2000JD900719, 2001.

Ver Hoef, J. M.: Who invented the delta method?, American Statistician, 66, 124–127, https://doi.org/10.1080/00031305.2012.687494, 2012.

Vicedo-Cabrera, A. M., Sera, F., Liu, C., Armstrong, B., Milojevic, A., Guo, Y. Y. L. L., Tong, S., Lavigne, E., Kyselý, J., Urban, A., Orru, H., Indermitte, E., Pascal, M., Huber, V., Schneider, A., Katsouyanni, K., Samoli, E., Stafoggia, M., Scortichini, M., Hashizume, M., Honda, Y., Ng, C. F. S., Hurtado-Diaz, M., Cruz, J., Silva, S., Madureira, J., Scovronick, N., Garland, R. M., Kim, H., Tobias, A., Íñiguez, C., Forsberg, B., Åström, C., Ragettli, M. S., Röösli, M., Guo, Y. Y. L. L., Chen, B. Y., Zanobetti, A., Schwartz, J., Bell, M. L., Kan, H., and Gasparrini, A.: Short term association between ozone and mortality: global two stage time series study in 406 locations in 20 countries, The BMJ, 368, 1–10, https://doi.org/10.1136/bmj.m108, 2020.

Wang, Y., Puthussery, J. V., Yu, H., Liu, Y., Salana, S., and Verma, V.: Sources of cellular oxidative potential of water-soluble fine ambient particulate matter in the Midwestern United States, Journal of Hazardous Materials, 425, 127 777, https://doi.org/10.1016/j.jhazmat.2021.127777, 2022.

Wegesser, T. C., Pinkerton, K. E., and Last, J. A.: California wildfires of 2008: Coarse and fine particulate matter toxicity, Environmental Health Perspectives, 117, 893–897, https://doi.org/10.1289/ehp.0800166, 2009.

Wei, Y., Wang, Y., Wu, X., Di, Q., Shi, L., Koutrakis, P., Zanobetti, A., Dominici, F., and Schwartz, J. D.: Causal effects of air pollution on mortality rate in Massachusetts, American Journal of Epidemiology, 189, 1316–1323, https://doi.org/10.1093/aje/kwaa098, 2020.

WHO: Health Risk Assessment of air pollution, World Health Organization, pp. 1–40, 2016.

WHO: WHO global air quality guidelines. Particulate matter (PM2.5 and PM10), ozone, nitrogen dioxide, sulfur dioxide and carbon monoxide, 2021.

Wiedinmyer, C., Akagi, S., Yokelson, R. J., Emmons, L., Al-Saadi, J., Orlando, J., and Soja, A.: The Fire INventory from NCAR (FINN): A high resolution global model to estimate the emissions from open burning, Geoscientific Model Development, 4, 625–641, 2011.

Willmott, C. J.: On the validation of models, Physical Geography, 2, 184–194, https://doi.org/10.1080/02723646.1981.10642213, 1981.

World Bank: Total population, https://data.worldbank.org/indicator/SP.POP.TOTL(Accessed11Dec.2021), 2020.

World Health Organization: Health risks of air pollution in Europe – HRAPIE project, World Heath Organization (WHO), p. 60, 2013.

Xie, Y., Lin, M., and Horowitz, L. W.: Summer PM2.5 Pollution Extremes Caused by Wildfires Over the Western United States During 2017–2018, Geophysical Research Letters, 47, 1–11, https://doi.org/10.1029/2020GL089429, 2020.

Xu, L., Crounse, J. D., Vasquez, K. T., Allen, H., Wennberg, P. O., Bourgeois, I., Brown, S. S., Campuzano-Jost, P., Coggon, M. M., Crawford, J. H., DiGangi, J. P., Diskin, G. S., Fried, A., Gargulinski, E. M., Gilman, J. B., Gkatzelis, G. I., Guo, H., Hair, J. W., Hall, S. R., Halliday, H. A., Hanisco, T. F., Hannun, R. A., Holmes, C. D., Huey, L. G., Jimenez, J. L., Lamplugh, A., Lee, Y. R., Liao, J., Lindaas, J., Neuman,

https://doi.org/10.5194/nhess-2023-111
Preprint. Discussion started: 18 July 2023




J. A., Nowak, J. B., Peischl, J., Peterson, D. A., Piel, F., Richter, D., Rickly, P. S., Robinson, M. A., Rollins, A. W., Ryerson, T. B., Sekimoto, K., Selimovic, V., Shingler, T., Soja, A. J., St. Clair, J. M., Tanner, D. J., Ullmann, K., Veres, P. R., Walega, J., Warneke, C., Washenfelder, R. A., Weibring, P., Wisthaler, A., Wolfe, G. M., Womack, C. C., and Yokelson, R. J.: Ozone chemistry in western U.S. wildfire plumes, Science Advances, 7, https://doi.org/10.1126/sciadv.abl3648, 2021.

Xu, R., Yu, P., Abramson, M. J., Johnston, F. H., Samet, J. M., Bell, M. L., Haines, A., Ebi, K. L., Li, S., and Guo, Y.: Wildfires, Global Climate Change, and Human Health, New England Journal of Medicine, 383, 2173–2181, https://doi.org/10.1056/NEJMsr2028985, 2020.

Zaveri, R. A., Easter, R. C., Fast, J. D., and Peters, L. K.: Model for simulating aerosol interactions and chemistry (MOSAIC), Journal of Geophysical Research: Atmospheres, 113, 2008.

Zhou, X., Josey, K., Kamareddine, L., Caine, M. C., Liu, T., Mickley, L. J., Cooper, M., and Dominici, F.: Excess of COVID-19 cases and deaths due to fine particulate matter exposure during the 2020 wildfires in the United States, Science Advances, 7, 1–12, https://doi.org/10.1126/sciadv.abi8789, 2021.